Published by
NIGERIAN SOCIETY OF PHYSICAL SCIENCES
Available online @ https://asr.nsps.org.ng/index.php/asr

African Scientific Reports 5 (2026) 617

African Scientific Reports

A mathematical model of typhoid fever–amebiasis co-infection dynamics with direct contact transmission mechanism

Kazeem A. Tijani[a], Agatha Abokwara[a,*], Olajide Theophilus Gomina[b], Olayiwola Timothy Apata[c], Aondongu Ignatius Chivir[d], Olorunfemi Ayodele Fakunle[e]

[a]*Department of Mathematics, Joseph Sarwan Tarka University, Makurdi, Benue State, Nigeria*
[b]*Department of Mathematics, Kogi State College of Education Technical, Mopa, Kogi State, Nigeria*
[c]*Department of Mathematics, Federal College of Education Okene, Kogi State, Nigeria*
[d]*Department of Statistics, Federal Polytechnic, Wannune, Benue State, Nigeria*
[e]*Department of Physics, Lagos State University, Lagos State, Nigeria*

Abstract

Amebiasis and typhoid fever are life-threatening tropical diseases that affect the human intestine and can lead to death. Both share a common transmission route and are prevalent in developing countries, particularly in regions with poor sanitation and hygiene. Consequently, concurrent infection is inevitable in such populations. This study investigates the transmission dynamics of amebiasis-typhoid co-infection by computing the reproduction number, stability, bifurcation, and sensitivity analyses. Simulation results further examine the impact of screening and treatment, showing that effective preventive measures, alongside adequate screening and treatment, are essential to control each disease and their co-infection.

DOI: 10.46481/asr.2026.5.3.617

Keywords: Amebiasis, Co-infection, Sensitivity analysis, Bifurcation, Typhoid fever

Article History:
Received: 31 July 2026
Received in revised form: 22 August 2026
Accepted for publication: 27 September 2026
Available online: 12 October 2026

© 2026 The Author(s). Published by the Nigerian Society of Physical Sciences under the terms of the Creative Commons Attribution 4.0 International license. Further distribution of this work must maintain attribution to the author(s) and the published article's title, journal citation, and DOI.

1. Introduction

Typhoid fever is a serious illness caused by *Salmonella Typhi*, transmitted primarily through contaminated food, water, or surfaces [1]. It is most common in populations lacking safe water and sanitation, particularly in Africa, Asia, and Latin America [2]. The incubation period ranges from 6 to 30 days [3]. In 2019, approximately 9 million cases and 110,000 deaths were reported globally, with antibiotics remaining the primary treatment [1].

Amebiasis denotes an intestinal parasitic infection attributable to *Entamoeba histolytica*. [4]. It is transmitted via the faecal–oral route through contaminated food, water, poor hygiene, contaminated surfaces, and, less commonly, sexual contact [5]. The incubation period typically ranges from 2 to 4 weeks. Symptoms include diarrhoea, abdominal pain, and cramping. In severe cases, the condition may progress to bloody stool, fever, and potentially death if not properly managed [4, 5]. Globally, it is the second

*Corresponding Author Tel. No.: +234-703-555-3966.
Email address: agathamicheal@gmail.com (Agatha Abokwara)

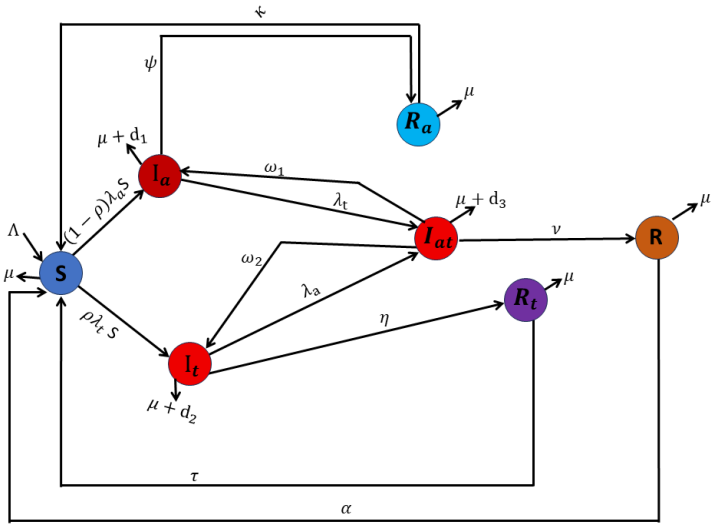


Figure 1: Typhoid fever–amebiasis co-dynamics flow diagram.

leading cause of death among parasitic diseases after malaria [6]. The infection remains endemic in many developing regions of Central and South America, Asia, and Africa, where access to potable water, proper hygiene, and adequate sanitation is limited [4, 7].

Amebiasis and typhoid fever are life-threatening intestinal diseases prevalent in tropical regions, both sharing similar transmission routes [5, 6]. They are widespread in developing countries, particularly where sanitation and hygiene are poor [1, 4, 5]. Consequently, concurrent infection is common in populations lacking adequate sanitation and hygiene [6].

Maxwell *et al.* [8] investigated water-related diseases in Benue State, Nigeria, analysing trends and spatial distribution, and reported cases of malaria, diarrhoea, dysentery, filariasis, onchocerciasis, amebiasis, schistosomiasis, typhoid fever, and cholera across all 23 local government areas. They recommended improved public education on hygiene and enhanced community water supply to control these diseases. Similarly, Jombo *et al.* [9] and Iboyi *et al.* [10] examined typhoid fever and amebiasis in Makurdi, respectively, providing insights into their transmission dynamics. Building on this established presence, the present study employs mathematical modelling to analyse typhoid–amebiasis co-infection using demographic data from Makurdi to propose effective control strategies.

Mathematical models are imperative for understanding disease transmission dynamics and guiding control interventions [11, 12]. While several studies have developed individual models for typhoid fever [13–15] and amebiasis [16–19], fewer have examined their co-infection in medical and clinical sciences, though valuable insights exist [6, 20, 21]. To the best of our knowledge, no author has used mathematical modelling to assess typhoid fever-amebiasis co-dynamics. Thus, this study applies mathematical modelling to investigate the spread of typhoid fever and its co-infection with amebiasis, incorporating screening and treatment as mechanisms to interrupt transmission. Accordingly, this study develops a seven-compartment co-infection model to analyse the dynamics of typhoid fever and amebiasis, with the aim of reducing their public health burden.

The study is organized as follows: Section 2 introduces the model formulation; Section 3 presents the qualitative analysis; Section 4 details the numerical simulations; and Sections 5 and 6 provide the discussion and conclusion.

2. Model formulation

Following the epidemiology of typhoid fever and amebiasis co-infection, the human population is partitioned into seven compartments: susceptible individuals, $S(t)$; amebiasis-infected individuals, I_a; typhoid fever-infected individuals, I_t; co-infected individuals, I_{at}; amebiasis-recovered individuals, R_a; typhoid fever-recovered individuals, R_t; and co-infection recovered individuals, R. The total population at time t is given by

$$N(t) = S + I_a + I_t + I_{at} + R_a + R_t + R.$$

The force of infection for amebiasis is defined as $\lambda_a = \beta_a(I_a + I_{at})$, and for typhoid fever as $\lambda_t = \beta_t(I_t + I_{at})$, where β_a and β_t denote the respective human-to-human contact rates.

Figure 1 illustrates the interaction and transition dynamics of typhoid-amebiasis co-infection across compartments, while Table 1 lists and describes all parameters. The human population is assumed to be homogeneous, with disease-related mortality occurring across all infected and infectious classes [1, 6]. Each infected compartment includes symptomatic, asymptomatic, or carrier individuals (in the case of typhoid fever). Transmission is restricted to the direct human-to-human route [1, 4]. By combining the

Table 1: Parameter descriptions.

Parameter	Description	Unit (day)	Value	Source
Λ	Recruitment rate	$\frac{\text{Human population}}{\text{time}}$	25	Estimated
$\rho \in (0,1)$	Proportion of individuals that become infected with typhoid fever	no unit	0.65	Assumed
d_1	Disease-related mortality rate for I_a individuals	time^{-1}	0.000055	[18]
d_2	Disease-related mortality rate for I_t individuals	time^{-1}	0.000286	[22]
d_3	Disease-related mortality rate for I_{at} individuals	time^{-1}	0.000341	Estimated
ψ	Progress rate from I_a to R_a due to screening and treatment	time^{-1}	0.133	[23]
η	Progress rate from I_t to R_t due to screening and treatment	time^{-1}	$\frac{1}{10}$	[24]
ω_2	Progress rate from I_{at} to I_t due to screening and treatment	time^{-1}	0.133	Assumed
ω_1	Progress rate from I_{at} to I_a due to screening and treatment	time^{-1}	0.1	[24]
ν	Progress rate from I_{at} to R due to screening and treatment	time^{-1}	0.1	Estimated
κ	Progress rate from R_a to S due to loss of immunity	time^{-1}	0.0667	Estimated [4, 6]
τ	Progress rate from R_t to S due to loss of immunity	time^{-1}	0.0667	Estimated [1, 3]
α	Progress rate from R to S due to loss of immunity	time^{-1}	0.0667	Estimated
μ	Human natural death rate	time^{-1}	0.000049	[25]
β_a	Amebiasis contact rate from human-to-human	1/person × time	0.00000164	Assumed
β_t	Typhoid fever contact rate from human-to-human	1/person × time	0.00000197	[26]

compartmental flow diagram in Figure 1 with the parameter descriptions in Table 1, the following system of equations is derived.

$$\left.\begin{aligned}
\frac{dS}{dt} &= \Lambda + \kappa R_a + \tau R_t + \alpha R - \rho\lambda_t S - (1-\rho)\lambda_a S - \mu S,\\
\frac{dI_a}{dt} &= (1-\rho)\lambda_a S + \omega_1 I_{at} - (\lambda_t + \psi + d_1 + \mu) I_a,\\
\frac{dI_t}{dt} &= \rho\lambda_t S + \omega_2 I_{at} - (\lambda_a + \eta + d_2 + \mu) I_t,\\
\frac{dI_{at}}{dt} &= \lambda_t I_a + \lambda_a I_t - (\nu + d_3 + \omega_1 + \omega_2 + \mu) I_{at},\\
\frac{dR_a}{dt} &= \psi I_a - (\kappa + \mu) R_a,\\
\frac{dR_t}{dt} &= \eta I_t - (\tau + \mu) R_t,\\
\frac{dR}{dt} &= \nu I_{at} - (\alpha + \mu) R.
\end{aligned}\right\} \tag{1}$$

where initial conditions, $S(0) > 0,\ I_a(0) > 0,\ I_t(0) > 0,\ I_at(0) > 0,\ R_a(0) \geq 0,\ R_t(0) \geq 0,\ R(0) \geq 0$, with $\lambda_a = \beta_a(I_a + I_{at}),\ \lambda_t = \beta_t(I_t + I_{at})$, with the model parameters taken to be non-negative.

3. Model qualitative analysis

This section examines the key features of system Eq. (1) by analysing the typhoid fever and amebiasis sub-models, with emphasis on the basic reproduction number and the stability of the disease-free equilibrium, and relates these results to the co-infection model.

3.1. Sub-model for typhoid fever

To obtain the typhoid fever sub-model from the system of equations Eq. (1), we set $\lambda_a = I_a = I_{at} = R_a = R = 0$ and this gives the typhoid fever sub-model as

$$\left.\begin{aligned}
\frac{dS}{dt} &= \Lambda + \tau R_t - \rho\lambda_t S - \mu S,\\
\frac{dI_t}{dt} &= \rho\lambda_t S - (\eta + d_2 + \mu) I_t,\\
\frac{dR_t}{dt} &= \eta I_t - (\tau + \mu) R_t,
\end{aligned}\right\} \tag{2}$$

with initial conditions, $S(0) > 0\ I_t(0) > 0,\ R_t(0) \geq 0, R(0) \geq 0$, where $\lambda_t = \beta_t I_t$, and assumed non-negative model parameters.

3.1.1. Typhoid fever sub-model invariant region

Here, the invariant region in which the system solutions lie is derived. The human population is $N(t) = S + I_t + R_t$, with initial condition $N(0) = N_0$.

Theorem 3.1. The feasible solutions of the model are uniformly bounded in the region

$$\Pi_{TF} = \Big\{(S, I_t, R_t) \in \mathbb{R}^3_+ : N(t) \leq \frac{\Lambda}{\mu}\Big\}.$$

Proof. From Eq. (2), we have

$$\frac{dN}{dt} = \Lambda - \mu N - d_2 I_t \leq \Lambda - \mu N,$$

when there is no disease related death, meaning, $d_2 = 0$. Applying integrating factor technique with $N(0) = N_0$ gives

$$N(t) \leq \frac{\Lambda}{\mu} + \Big(N_0 - \frac{\Lambda}{\mu}\Big)e^{-\mu t}. \tag{3}$$

As $t \longrightarrow \infty$ in Eq. (3), $N(t) \leq \frac{\Lambda}{\mu}$, implying the feasible solution of equation Eq. (2) is in the region,

$$\Pi_{TF} = \Big\{(S, I_t, R_t) \in \mathbb{R}^3_+ : N(t) \leq \frac{\Lambda}{\mu}\Big\}.$$

Thus, the feasible region for the model system of Eq. (2) is given by $\Pi_{TF} = \Big\{(S, I_t, R_t) \in \mathbb{R}^3_+ : N(t) \leq \frac{\Lambda}{\mu}\Big\}$. Hence, since the initial conditions of the state variables are non-zero and the parameters are positive together with this invariant region obtained, it implies that the sub-model of the typhoid fever is universally valid. So, it implies that model Eq. (2) in this region Π_{TF} can be studied. □

3.2. Stability of TFFE and typhoid fever reproduction number R_0^t

The TFFE, typhoid fever-free equilibrium is obtained when $I_t = R_t = 0$. Thus,

$$TFFE(E_0^t) = (S_0, I_{t0}, R_{t0}) = \Big(\frac{\Lambda}{\mu},\ 0,\ 0\Big).$$

Following the approach of Van den Driessche & Watmough [27] as adopted by Ref. [28], the basic reproduction number for typhoid fever, R_0^t, in system Eq. (2) is computed as the spectral radius (maximum eigenvalue) of FV^{-1}. Here, $F = (\rho\beta_t S_0)$ represents the matrix of new infection rates in the infected compartment, while $V = (\eta + d_2 + \mu)$ denotes the matrix of transition terms accounting for non-new infections, i.e., transfers between compartments. Hence, the typhoid basic reproduction number is obtained as

$$R_0^t = \frac{\rho\beta_t\Lambda}{\mu(\eta + d_2 + \mu)}.$$

This represent the number of secondary cases of typhoid fever infection that can be produced from the proportion, ρ at the contact rate, β_t, in a population size, $\frac{\Lambda}{\mu}$ over the period of $\frac{1}{\eta+d_2+\mu}$.

3.2.1. Local stability of typhoid fever-free equilibrium (TFFE)

Theorem 3.2. The TFFE E_0^t of the typhoid fever sub-model, is locally asymptotically stable if $R_0^t < 1$, otherwise it is unstable if $R_0^t > 1$.

Proof. The Jacobian matrix of the sub-model Eq. (2) computed at E_0^t is given by

$$J(E_0^t) = \begin{pmatrix} -\mu & -\rho\beta_t S_0 & \tau \\ 0 & \rho\beta_t S_0 - (\eta + d_2 + \mu) & 0 \\ 0 & \eta & -(\tau + \mu) \end{pmatrix}.$$

By applying the inspection technique, the Jacobian matrix , $J(E_0^t)$, is found to have eigenvalues, $-\mu,\ -(\tau+\mu)$ and $(\eta+d_2+\mu)(R_0^t - 1)$. This implies that $J(E_0^t$ possesses negative real eigenvalues whenever $R_0^t < 1$. Therefore, the TFFE, E_0^t, is locally asymptotically stable if $R_0^t < 1$. Hence, the proof. □

3.2.2. Global stability of typhoid fever-free equilibrium (TFFE)

The following theorem demonstrates the global stability of the typhoid fever-free equilibrium point, E_0^t.

Theorem 3.3. The TFFE E_0^t of the typhoid fever sub-model Eq. (2), is locally asymptotically stable if $R_0^t < 1$, otherwise it is unstable if $R_0^t > 1$.

Proof. Following Castillo-Chavez & Song [29], the typhoid fever-free equilibrium is globally asymptotically stable when $R_0^t < 1$, provided two additional conditions are satisfied. These conditions are outlined below.

i. $F(X_1, 0)$ establishes a globally asymptotically stable equilibrium for $\frac{dX_1}{dt}$.

ii. Define $G(X_1, Y_1) = AY - G^*(X_1, Y_1)$, with $G(X_1, Y_1) \geq 0$ for all $X_1, Y_1 \in Q$. Here, $A = D_Y G(X^*, 0)$ is an M-matrix representing infected classes, and Π_{TF} denotes the biologically feasible region of the model.

To decompose system Eq. (2) into subsystems. Let $X_1 = (S)$ denote the population of uninfected humans, and define $Y_1 = (I_t)$ as the infected compartments with $R_t = 0$. Under these definitions, system Eq. (2) is reformulated as follows:

$$\left.\begin{aligned} \frac{dX_1}{dt} &= F(X_1, Y_1) \\ \frac{dY_1}{dt} &= G(X_1, Y_1) \end{aligned}\right\},$$

where $X_1 \in \mathbb{R}_+, Y_1 \in \mathbb{R}_+$. So, the functions of the two vector-valued are given thus.

$$\left.\begin{aligned} F(X_1, Y_1) &= \Big(\Lambda + \tau R_t - \rho\lambda_t S - \mu S, \Big)^T \\ G(X_1, Y_1) &= \Big(\rho\lambda_t S - (\eta + d_2 + \mu) I_t\Big)^T \end{aligned}\right\}.$$

T is the transpose. For convenience, we treat X_1 as equivalent to $(X_1, 0)$ and Y_1 with $(0, Y_1) \in \mathbb{R}_+ \times \mathbb{R}_+$ Hence. $\frac{dX_1}{dt} = F(X_1, 0)$ is

$$\frac{dS}{dt} = \Big(\Lambda + \tau R_t - \rho\lambda_t S - \mu S\Big). \tag{4}$$

The Jacobian matrix of subsystem Eq. (4) is $J(x^*) = \Big(-\mu\Big)$, with eigenvalue $-\mu$. Implying equilibrium point for the system $\frac{dX_1}{dt}, F(X_1, 0)$ exhibits global asymptotic stability as utilised by Ref. [29]. For the second condition

$$G(X_1, Y_1) = AY - G^*(X_1, Y_1),$$

with $G(X_1, Y_1) \geq 0$ for all $X_1, Y_1 \in Q$, where $A = D_Y G(X^*, 0)$ is an M-matrix. Clearly, $G(X_1, Y_1)$ satisfies

$$G(X_1, 0) = 0, \quad G(X_1, Y_1) = A^* Y_1 - G^*(X_1, Y_1), \quad G^*(X_1, Y_1) \geq 0,$$

with

$$A^* = D_Y G(X_1, 0) = \Big[\rho\beta_t S_0 - (\eta + d_2 + \mu)\Big].$$

and

$$G^*(X_1, Y_1) = \left[\rho\beta_t I_t \left(\frac{\Lambda}{\mu} - S\right)\right].$$

Since the population of humans attains a stable equilibrium value,

$$\rho\beta_t I_t \left(\frac{\Lambda}{\mu} - S\right) \geq 0, \quad \frac{\Lambda}{\mu} \geq S.$$

It follows that the typhoid fever sub-model is globally asymptotically stable, implying that the disease will eventually disappear regardless of the initial number of infected individuals. From an epidemiological perspective, this indicates that typhoid fever will be eliminated from the population in the absence of external interventions, provided the stability conditions of the disease-free equilibrium are maintained. □

3.2.3. Existence of endemic equilibrium (EE) state of the typhoid fever sub-model (EETF)

We establish the EE of the typhoid fever sub-model Eq. (2), representing a state in which infection remains in society. The equilibrium is given by

$$E^e = (S^e, I_t^e, R_t^e).$$

To determine E^e, the R.H.S of system Eq. (2) is set to zero and solved. Upon solving the system of equations Eq. (2), we have

$$S^e = \frac{\Lambda}{\mu R_0^t}, I_t^e = \frac{(\eta + d_2 + \mu)(\tau + \mu)(R_0^t - 1)}{\rho\beta_t((\eta + d_2 + \mu)(\tau + \mu) - \tau\eta)}, R_t^e = \frac{(\eta + d_2 + \mu)\eta(R_0^t - 1)}{\rho\beta_t((\eta + d_2 + \mu)(\tau + \mu) - \tau\eta)}.$$

For $S^e > 0, I_t^e > 0, R_t^e > 0$ provided $R_0^t > 1$. This existence of the endemic equilibrium of typhoid fever indicates the continued presence of typhoid fever in the population.

3.2.4. Bifurcation analysis of the typhoid fever sub-model

A crucial threshold, called bifurcation, is analysed to evaluate the impact of specific factors on typhoid fever transmission, particularly when the basic reproduction number, $R_{0t} = 1$. In the case of a backward bifurcation, the disease may persist in multiple steady states even when $R_{0t} < 1$, thereby complicating efforts to forecast and control the disease [30]. The centre manifold theorem [31] is applied to conduct the bifurcation analysis of system Eq. (2), with

$$a = \sum_{k,i,j=1}^{n} z_k w_i w_j \frac{\partial^2 f_k(E^0)}{\partial x_i \partial x_j}, \quad b = \sum_{k,i=1}^{n} z_k w_i \frac{\partial^2 f_k(E^0)}{\partial x_i \partial \beta_t},$$

serving as the bifurcation coefficients, and β_t as the bifurcation parameter. The condition $R_0^t = 1$ [32] holds if and only if

$$\beta_t = \beta_t^* = \frac{\mu(\mu + d_2 + \eta)}{\rho\Lambda}.$$

Such that $S = x_1, I_t = x_2, R_t = x_3$. Utilising vector notation $\vec{x} = (x_1, x_2, x_3)^T$, typhoid fever sub-model Eq. (2) can be written in the form $\vec{x}' = F(\vec{x})$, such that $F = (f_1, f_2, f_3)^T$, written below as

$$\left.\begin{aligned} \frac{dx_1}{dt} &= \Lambda + \tau x_3 - \rho\beta_t x_2 x_1 - \mu x_1, \\ \frac{dx_2}{dt} &= \rho\beta_t x_2 x_1 - (\eta + d_2 + \mu)x_2, \\ \frac{dx_3}{dt} &= \eta x_2 - (\tau + \mu)x_3, \end{aligned}\right\} \tag{5}$$

assuming non-negative initial conditions, the technique relies on the Jacobian of system Eq. (5) evaluated at the disease-free equilibrium, $J(E_0^t)$, have a simple zero eigenvalue and all other eigenvalues negative at $R_0^t = 1$

with eigenvalues w and z of $J(E_0^t)$ derived respectively utilising $J(E_0^t) \cdot w = 0$ and $J(E_0^t) \cdot z = 0$.

$$w_1 = \frac{[-\rho\beta_t S_0(\tau + \mu) + \tau\eta]w_2}{\mu(\mu + \tau)} < 0, w_3 = \frac{\eta w_2}{(\mu + \tau)}, \; w_2 = w_2 > 0, \tag{6}$$

$z_2 = z_2 > 0$,

$$z_1 = -\frac{[(\tau + \mu)(\rho\beta_t S_{h0} - (\eta + d_2 + \mu)) + \eta\tau]z_2}{(\tau + \mu)\rho\beta_t S_0} < 0, z_3 = -\frac{\tau z_2}{(\tau + \mu)}, \tag{7}$$

with $w.z = 1$, $\vec{w} = (w_1, w_2, w_3)^T$ and $\vec{z} = (z_1, z_2, z_3)^T$.

The non-zero second order derivatives of x_1, x_2, x_3 at disease-free equilibrium yield

$$\frac{\partial^2 f_1(E_0^t)}{\partial x_1 \partial x_2} = -\rho\beta_t, \; \frac{\partial^2 f_2(E_0^t)}{\partial x_1 \partial x_2} = \rho\beta_t, \tag{8}$$

and

$$z_1 w_2 \frac{\partial^2 f_1(E_0^t)}{\partial x_2 \partial \beta_t} = -z_1 w_2 \rho S_0, \; z_2 w_2 \frac{\partial^2 f_2(E_0^t)}{\partial x_2 \partial \beta_t} = z_2 w_2 \rho S_0. \tag{9}$$

Therefore, by using the non-zero second-order partial derivatives of equation Eq. (8) and equation Eq. (9), and given that $w.z = 1$, we obtain

$$a = -z_2 w_2^2 \left[\left(\frac{[(\tau+\mu)(\rho\beta_t S_0 - (\eta + d_2 + \mu)) + \eta\tau]}{(\tau+\mu)\rho\beta_t S_0} \right) \left(\frac{[-\rho\beta_t S_0(\tau+\mu) + \tau\eta]}{\mu(\mu+\tau)} \right) \rho\beta_t + \frac{[-\rho\beta_t S_0(\tau+\mu) + \tau\eta]}{\mu(\mu+\tau)} \right],$$

which gives

$$a = -z_2 w_2^2 \left[\left(\frac{2\tau\eta\beta_t\rho}{\mu(\mu+\tau)} + \frac{\rho\beta_t(\eta+d+\mu)}{\mu^2} + \frac{\eta^2\tau^2}{\Lambda(\mu+\tau)^2} \right) - \left(\frac{2\rho^2\beta_t^2\Lambda}{\mu^2} + \frac{\eta\rho\beta_t^2}{\mu(\mu+\tau)} + \frac{\tau\mu(\eta+d+\mu)}{\Lambda(\mu+\tau)} \right) \right].$$

Thus,

$$a > 0, \text{ if } \left(\frac{2\tau\eta\beta_t\rho}{\mu(\mu+\tau)} + \frac{\rho\beta_t(\eta+d+\mu)}{\mu^2} + \frac{\eta^2\tau^2}{\Lambda(\mu+\tau)^2} \right) < \left(\frac{2\rho^2\beta_t^2\Lambda}{\mu^2} + \frac{\eta\rho\beta_t^2}{\mu(\mu+\tau)} + \frac{\tau\mu(\eta+d+\mu)}{\Lambda(\mu+\tau)} \right) \tag{10}$$

and

$$a < 0, \text{ if } \left(\frac{2\tau\eta\beta_t\rho}{\mu(\mu+\tau)} + \frac{\rho\beta_t(\eta+d+\mu)}{\mu^2} + \frac{\eta^2\tau^2}{\Lambda(\mu+\tau)^2} \right) > \left(\frac{2\rho^2\beta_t^2\Lambda}{\mu^2} + \frac{\eta\rho\beta_t^2}{\mu(\mu+\tau)} + \frac{\tau\mu(\eta+d+\mu)}{\Lambda(\mu+\tau)} \right). \tag{11}$$

Also,

$$b = \rho S_0 z_2 w_2 \left[\frac{[(\tau+\mu)(\rho\beta_t S_0 - (\eta + d_2 + \mu)) + \eta\tau]}{(\tau+\mu)\rho\beta_t S_0} + 1 \right]. \tag{12}$$

This result in

$$b = \rho w_2 z_2 \frac{\Lambda}{\mu} \left[2 + \frac{\mu\eta\tau}{(\tau+\mu)\beta_t\Lambda\rho} - \frac{\mu(\eta+d_2+\mu)}{\rho\beta_t\Lambda} \right].$$

$$b > 0, \text{ if } \frac{\mu(\eta+d_2+\mu)}{\rho\beta_t\Lambda} \leq 2 \tag{13}$$

and

$$b < 0, \text{ if } 2 + \frac{\mu\eta\tau}{(\tau+\mu)\beta_t\Lambda\rho} < \frac{\mu(\eta+d_2+\mu)}{\rho\beta_t\Lambda}. \tag{14}$$

If equations Eq. (10) and Eq. (13) hold, then the system exhibits a backward bifurcation implying that the system support several stable equilibrium states of disease free and endemic equilibria implying that, $R_0^t < 1$ does not guarantee disease elimination from the population. On the other hand, if equations Eq. (11) and Eq. (13) hold, the system exhibits a forward bifurcation, hence, for $R_0^t < 1$, typhoid fever would be eliminated from the population [30]. Thus, Figure 2 depicts the resulting bifurcation diagram. Illustration from Figure 2 reveals that typhoid fever sub-model undergoes forward bifurcation. Hence, the TFFE displays global stability, illustrating the possibility of disease elimination and reduced transmission risk when the reproduction number, R_0^t remains below 1. Conversely, when the R_0^t exceeds one, the EE persists, leading to sustained spread.

3.3. Global stability of the endemic equilibrium state of the typhoid fever sub-model

We examine the global stability of the endemic equilibrium E^e to determine whether the system converges to this state for all admissible initial conditions within the feasible region. To establish this, we state and prove the following theorem.

Theorem 3.4. For $R_0^t > 1$, the endemic equilibrium state is globally asymptotically stable.

Proof. Let

$$V(X) = (S, I_t, R_t)^T.$$

Consider the Lyapunov function,

$$V(X) = \left[S - S^e - S^e \ln \frac{S}{S^e} \right] + a_1 \left[I_t - I_t^e - I_t^e \ln \frac{I_t}{I_t^e} \right] + a_2 \left[R_t - R_t^e - R_t^e \ln \frac{R_t}{R_t^e} \right], \tag{15}$$

where a_1 and a_2 are unknown constants. Thus, equation Eq. (15) becomes

$$V' = \left[1 - \frac{S^e}{S} \right] S' + a_1 \left[1 - \frac{I_t^e}{I_t} \right] I_t' + a_2 \left[1 - \frac{R_t^e}{R_t} \right] R_t'. \tag{16}$$

Let

$$\Lambda = -\tau R_t^e + \rho\beta_t I_t^e S^e + \mu S^e, \quad (\tau + d_2 + u) = \rho\beta_t S^e, \quad (\tau+\mu) = \frac{\eta I_t^e}{R_t^e}. \tag{17}$$

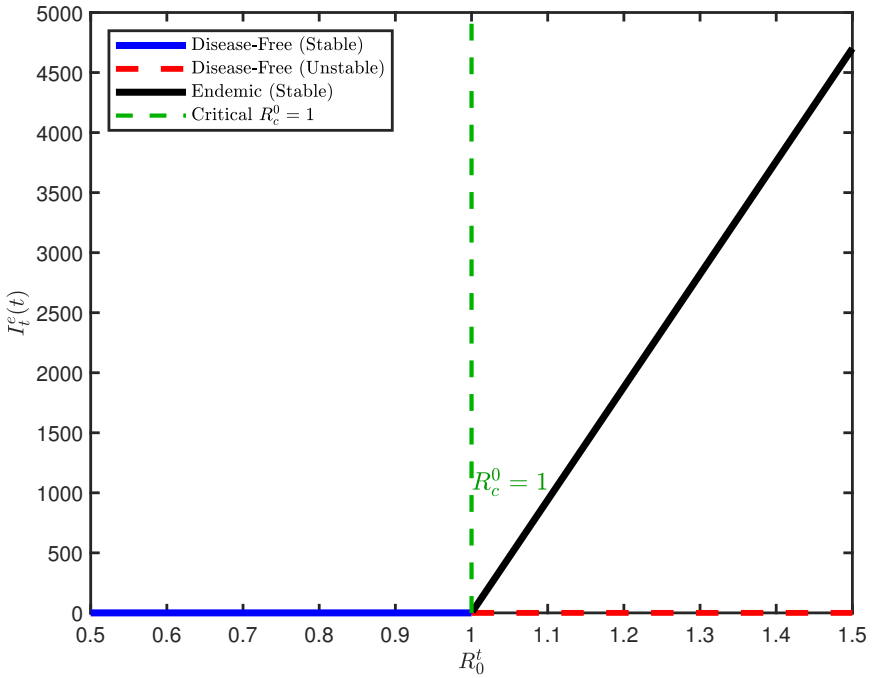


Figure 2: Bifurcation plot of the typhoid fever sub-model.

Substituting equation Eq. (17) into equation Eq. (16) result in

$$V' = -\mu\frac{(S - S^e)^2}{S} + \Big[1 - \frac{S^e}{S}\Big]\Big[\tau R_t^e\Big(\frac{R_t}{R_t^e} - 1\Big) + \rho\beta_t I_t^e S^e\Big(1 - \frac{S}{S^e}\frac{I_t}{I_t^e}\Big)\Big] + a_1\Big[1 - \frac{I_t^e}{I_t}\Big]\Big[\rho\beta_t I_t^e S^e$$
$$\Big(\frac{S}{S^e}\frac{I_t}{I_t^e} - 1\Big) + \rho\beta_t S^e I_t^e\Big(1 - \frac{I_t}{I_t^e}\Big)\Big] + a_2\Big[1 - \frac{R_t^e}{R_t}\Big]\Big[\eta I_t^e\Big(\frac{I_t}{I_t^e} - 1\Big) + \eta I_t^e\Big(1 - \frac{R_t}{R_t^e}\Big)\Big]. \tag{18}$$

The coefficients of $\frac{S}{S^e}$, $\frac{I_t}{I_t^e}$, and $\frac{R_t}{R_t^e}$ are chosen such that $a_1 = 1$, $a_2 = \frac{\tau R_t^e}{\eta I_t^e}$ and $\rho\beta_t I_t^e S^e = 0$. Thus equation Eq. (18) becomes

$$V' = -\mu\frac{(S - S^e)^2}{S} + \tau R_t^e\Big[-\frac{R_t}{R_t^e}\cdot\frac{S^e}{S} + \frac{S^e}{S} + \frac{I_t}{I_t^e} - \frac{I_t}{I_t^e}\cdot\frac{R_t^e}{R_t}\Big] + \rho\beta_t S^e\Big[2 - \frac{I_t}{I_t^e} - \frac{I_t^e}{I_t}\Big]. \tag{19}$$

Consider the function $v(x) = 1 - x > 0$, with equality attained only at $x = 1$. Since $1 - x \le -\ln x$, it follows that the τR_t^e term in equation Eq. (19) reduces to

$$\Big(1 - \frac{R_t}{R_t^e}\cdot\frac{S^e}{S}\Big) - \Big(1 - \frac{S^e}{S}\Big) + \Big(1 - \frac{I_t}{I_t^e}\cdot\frac{R_t^e}{R_t}\Big) - \Big(1 - \frac{I_t}{I_t^e}\Big) \le -\ln\frac{R_t}{R_t^e}\cdot\frac{S^e}{S} + \ln\frac{S^e}{S} - \ln\frac{I_t}{I_t^e}\cdot\frac{R_t^e}{R_t} + \ln\frac{I_t}{I_t^e}$$
$$= \ln\Big(\frac{S}{S^e}\cdot\frac{R_t^e}{R_t}\cdot\frac{S^e}{S}\cdot\frac{R_t}{R_t^e}\cdot\frac{I_t^e}{I_t}\cdot\frac{I_t}{I_t^e}\Big) = 0.$$

Also, using arithmetic-geometric mean on the $\rho\beta_t S^e$ term in equation Eq. (19) gives zero. Thus, equation Eq. (19) becomes

$$V' = -\mu\frac{(S - S^e)^2}{S} \le 0. \tag{20}$$

By applying LaSalle's invariance principle [33], we conclude that the solutions of the typhoid sub-model Eq. (2) converge to the endemic equilibrium for $R_0^t > 1$ as $t \to \infty$. Hence, the unique endemic equilibrium of the typhoid fever sub-model Eq. (2) is globally asymptotically stable. □

3.4. Amebiasis sub-model

By setting the state variables and parameters associated with typhoid fever to zero, we obtain the amebiasis sub-model:

$$\left.\begin{aligned} \frac{dS}{dt} &= \Lambda + \kappa R_a - (1-\rho)\lambda_a S - \mu S, \\ \frac{dI_a}{dt} &= (1-\rho)\lambda_a S - (\psi + d_1 + \mu) I_a, \\ \frac{dR_a}{dt} &= \psi I_a - (\kappa + \mu) R_a, \end{aligned}\right\} \tag{21}$$

with initial conditions $S(0) > 0,\ I_a(0) > 0,\ R_a(0) \geq 0$, where $\lambda_a = \beta_a I_a$ and $N = S + I_a + R_a$. Analogously, the domain of feasible solutions for the amebiasis sub-model, representing the human population, is given by

$$\Pi_A = \left\{(S,\ I_a,\ R_a) \in \mathbb{R}^3_+ : N \leq \frac{\Lambda}{\mu}\right\}.$$

This region Π_A is positively invariant. Hence, the amebiasis system Eq. (21) is both epidemiologically and mathematically well-posed, justifying its study within the domain Π_A.

3.4.1. Amebiasis-free equilibrium (AFE) and amebiasis basic reproduction number, R_0^a

The amebiasis-free equilibrium (AFE) is obtained by setting $I_a = R_a = 0$ in equation Eq. (21). Thus,

$$E_0^a = (S_0, I_{a0}, R_{a0}) = \left(\tfrac{\Lambda}{\mu}, 0, 0\right).$$

Following the same approach, the basic reproduction number R_0^a for system (21) is computed as

$$R_0^a = \frac{\Lambda(1-\rho)\beta_a}{\mu(\psi + d_1 + \mu)}.$$

This quantity represents the expected number of secondary amebiasis cases generated from the susceptible fraction $(1-\rho)$, at contact rate β_a, over the average infectious period $\frac{1}{\psi+d_1+\mu}$.

Local stability of amebiasis-free equilibrium (AFE)

Theorem 3.5. The AFE E_0^a of system Eq. (21) is locally asymptotically stable if $R_0^a < 1$, otherwise it is not stable if $R_0^a > 1$.

Proof. The Jacobian matrix of system Eq. (21) evaluated at the amebiasis-free equilibrium E_0^a is

$$J(E_0^a) = \begin{pmatrix} -\mu & -(1-\rho)\beta_a S_0 & \kappa \\ 0 & (1-\rho)\beta_a S_0 - (\psi + d_1 + \mu) & 0 \\ 0 & \psi & -(\kappa + \mu) \end{pmatrix}.$$

By inspection, the eigenvalues of $J(E_0^a)$ are $-\mu,\ -(\kappa+\mu)$, and $(\psi+d_1+\mu)(R_0^a-1)$. It follows that all eigenvalues are negative whenever $R_0^a < 1$. Therefore, the equilibrium E_0^a is locally asymptotically stable if $R_0^a < 1$. Hence, the result is established. □

Global stability of amebiasis-free equilibrium (AFE)

The following theorem demonstrates the global stability of the amebiasis-free equilibrium point, E_0^a.

Theorem 3.6. The amebiasis-free equilibrium (AFE) E_0^a of the sub-model Eq. (21) is globally asymptotically stable when $R_0^a < 1$, and unstable when $R_0^a > 1$.

Proof. As noted by Castillo-Chavez *et al.* [29], if the amebiasis-free equilibrium is locally asymptotically stable for $R_0^a < 1$, two additional conditions must be satisfied to guarantee global stability:

i. $F(X_1, 0)$ defines a globally asymptotically stable equilibrium for $\frac{dX_1}{dt}$.

ii. $G(X_1, Y_1) = AY - G^*(X_1, Y_1)$, with $G(X_1, Y_1) \geq 0$ for all $X_1, Y_1 \in Q$, where $A = D_Y G(X^*, 0)$ is an M-matrix of infected classes and Π_A denotes the biologically feasible region.

To verify these conditions, we introduce new variables and decompose system (21). Let $X_1 = (S)$ represent the susceptible population and $Y_1 = (I_a)$ the infected compartments, with $R_a = 0$. The system becomes

$$\frac{dX_1}{dt} = F(X_1, Y_1), \quad \frac{dY_1}{dt} = G(X_1, Y_1),$$

where $X_1, Y_1 \in \mathbb{R}_+$. Explicitly,

$$F(X_1, Y_1) = \big(\Lambda + \kappa R_a - (1-\rho)\lambda_a S - \mu S\big)^T,$$
$$G(X_1, Y_1) = \big((1-\rho)\lambda_a S - (\psi + d_1 + \mu)I_a\big)^T.$$

For the reduced system $\frac{dX_1}{dt} = F(X_1, 0)$, we obtain

$$\frac{dS}{dt} = \Lambda + \kappa R_a - (1-\rho)\lambda_a S - \mu S,$$

with Jacobian

$$J(x^*) = (-\mu),$$

which has eigenvalue $-\mu < 0$. Thus, $F(X_1, 0)$ is globally asymptotically stable [29]. For condition (ii), $G(X_1, Y_1)$ satisfies $G(X_1, 0) = 0$ and can be expressed as

$$G(X_1, Y_1) = A^* Y_1 - G^*(X_1, Y_1), \quad G^*(X_1, Y_1) \geq 0,$$

where

$$A^* = D_Y G(X_1, 0) = (\rho\beta_t S_0 - (\psi + d_1 + \mu)),$$
$$G^*(X_1, Y_1) = \big((1-\rho)\beta_a I_a(\tfrac{\Lambda}{\mu} - S)\big).$$

Since the human population approaches the steady-state $\frac{\Lambda}{\mu} \geq S$, it follows that $(1-\rho)\beta_a I_a(\frac{\Lambda}{\mu} - S) \geq 0$. Therefore, the amebiasis sub-model satisfies both conditions, establishing global asymptotic stability. This implies that amebiasis can be eradicated regardless of the initial number of infected individuals. □

3.4.2. Existence of endemic equilibrium (EE) state of the amebiasis sub-model (EEA)

The EE of the amebiasis sub-model Eq. (21) characterizes the persistence of infection within the population. It is defined as

$$E^{e*} = (S^{e*}, I_a^{e*}, R_a^{e*}).$$

The equilibrium is obtained by setting the R.H.S of system Eq. (21) to zero, yielding

$$S^{e*} = \frac{\Lambda}{\mu R_0^a}, \quad I_a^{e*} = \frac{(\psi + d_1 + \mu)(\kappa + \mu)(R_0^a - 1)}{(1-\rho)\beta_a((\psi + d_1 + \mu)(\kappa + \mu) - \psi\kappa)}, \quad R_a^{e*} = \frac{(\psi + d_1 + \mu)\eta(R_0^a - 1)}{(1-\rho)\beta_a((\psi + d_1 + \mu)(\kappa + \mu) - \psi\kappa)}.$$

Existence of the endemic equilibrium requires $R_0^a > 1$, ensuring persistence of amebiasis within the population.

3.4.3. Bifurcation analysis of the amebiasis sub-model

To analyse the bifurcation behaviour of system Eq. (21) , we apply the Centre Manifold Theorem of Castillo-Chavez & Song [31]. The bifurcation coefficients take the form

$$a = \sum_{k,i,j=1}^{n} z_k w_i w_j \frac{\partial^2 f_k(E_0^a)}{\partial x_i \partial x_j}, \quad b = \sum_{k,i=1}^{n} z_k w_i \frac{\partial^2 f_k(E_0^a)}{\partial x_i \partial \beta_a},$$

where β_a serves as the bifurcation parameter. The threshold condition $R_0^a = 1$ [32] holds if and only if

$$\beta_a = \beta_a^* = \frac{\mu(\mu + d_1 + \psi)}{(1-\rho)\Lambda}.$$

Such that $S = x_1, I_a = x_2, R_a = x_3$. Using vector notation $\vec{x} = (x_1, x_2, x_3)^T$, the amebiasis sub-model Eq. (21) is expressed as $\vec{x}' = F(\vec{x})$, where $F = (f_1, f_2, f_3)^T$, as shown below.

$$\left.\begin{aligned} \frac{dx_1}{dt} &= \Lambda + \kappa x_3 - (1-\rho)\lambda_a x_1 - \mu x_1, \\ \frac{dx_2}{dt} &= (1-\rho)\lambda_a x_1 - (\psi + d_1 + \mu)x_2, \\ \frac{dx_3}{dt} &= \psi x_2 - (\kappa + \mu)x_3, \end{aligned}\right\} \tag{22}$$

with non-negative initial conditions. By Centre Manifold Theorem [31], bifurcation analysis of system Eq. (22) requires that the Jacobian at the disease-free equilibrium, $J(E_0^a)$, exhibit a simple zero eigenvalue, with the rest strictly negative when $R_0^a = 1$. The corresponding right and left eigenvectors, w and z, are obtained from $J(E_0^a) \cdot w = 0$ and $J(E_0^a) \cdot z = 0$, respectively, and are given by

$$w_1 = \frac{[-(1-\rho)\beta_a S_0(\kappa+\mu) + \kappa\psi]w_2}{\mu(\mu+\kappa)} < 0, \quad w_2 > 0, \quad w_3 = \frac{\psi w_2}{\mu+\kappa},$$

$$z_1 = -\frac{[(\kappa+\mu)(\rho\beta_a S_0 - (\kappa+d_1+\mu)) + \psi\kappa]z_2}{(\kappa+\mu)(1-\rho)\beta_a S_0} < 0, \quad z_2 > 0, \quad z_3 = -\frac{\kappa z_2}{\kappa+\mu},$$

with normalization $w \cdot z = 1$, where $\vec{w} = (w_1, w_2, w_3)^T$ and $\vec{z} = (z_1, z_2, z_3)^T$. The second-order derivatives at the disease-free equilibrium that are non-zero are

$$\frac{\partial^2 f_1(E_0^a)}{\partial x_1 \partial x_2} = -(1-\rho)\beta_a, \quad \frac{\partial^2 f_2(E_0^a)}{\partial x_1 \partial x_2} = (1-\rho)\beta_a,$$

and

$$z_1 w_2 \frac{\partial^2 f_1(E_0^a)}{\partial x_2 \partial \beta_a} = -z_1 w_2 (1-\rho) S_0, \quad z_2 w_2 \frac{\partial^2 f_2(E_0^a)}{\partial x_2 \partial \beta_a} = z_2 w_2 (1-\rho) S_0.$$

Using these derivatives, the bifurcation coefficients are computed as

$$a = -(1-\rho)\beta_a w_2^2 z_2 \Big[\left(\frac{\beta_a \Lambda}{\mu^2} + \frac{\psi\kappa}{(\kappa+\mu)} + \frac{\psi\kappa(\kappa+d_1+\mu)}{\Lambda\beta_a(\mu+\kappa)(1-\rho)} \right) - \left((k+d_1+\mu) + \frac{\kappa\psi}{\mu(\mu+\kappa)} + \frac{\rho\kappa\psi}{\mu(\mu+\kappa)(1-\rho)} + \frac{\kappa^2\psi^2}{(\kappa+\mu)^2(1-\rho)\beta_a\Lambda} \right) \Big].$$

$a > 0$, if

$$\left(\frac{\beta_a \Lambda}{\mu^2} + \frac{\psi\kappa}{(\kappa+\mu)} + \frac{\psi\kappa(\kappa+d_1+\mu)}{\Lambda\beta_a(\mu+\kappa)(1-\rho)} \right) < \left((k+d_1+\mu) + \frac{\kappa\psi}{\mu(\mu+\kappa)} + \frac{\rho\kappa\psi}{\mu(\mu+\kappa)(1-\rho)} + \frac{\kappa^2\psi^2}{(\kappa+\mu)^2(1-\rho)\beta_a\Lambda} \right) \tag{23}$$

and $a < 0$, if

$$\left(\frac{\beta_a \Lambda}{\mu^2} + \frac{\psi\kappa}{(\kappa+\mu)} + \frac{\psi\kappa(\kappa+d_1+\mu)}{\Lambda\beta_a(\mu+\kappa)(1-\rho)} \right) > \left((k+d_1+\mu) + \frac{\kappa\psi}{\mu(\mu+\kappa)} + \frac{\rho\kappa\psi}{\mu(\mu+\kappa)(1-\rho)} + \frac{\kappa^2\psi^2}{(\kappa+\mu)^2(1-\rho)\beta_a\Lambda} \right). \tag{24}$$

For b, we have

$$b = (1-\rho)\frac{\Lambda}{\mu} w_2 z_2 \left[\left(1 + \frac{\rho}{1-\rho} + \frac{\psi\kappa\mu}{(\kappa+\mu)(1-\rho)\beta_a\Lambda} \right) - \frac{\mu(\kappa+d_1+\mu)}{\Lambda\beta_a(1-\rho)} \right].$$

Also, $b < 0$, if

$$\left(1 + \frac{\rho}{1-\rho} + \frac{\psi\kappa\mu}{(\kappa+\mu)(1-\rho)\beta_a\Lambda} \right) < \frac{\mu(\kappa+d_1+\mu)}{\Lambda\beta_a(1-\rho)} \tag{25}$$

and $b > 0$, if

$$\left(1 + \frac{\rho}{1-\rho} + \frac{\psi\kappa\mu}{(\kappa+\mu)(1-\rho)\beta_a\Lambda} \right) > \frac{\mu(\kappa+d_1+\mu)}{\Lambda\beta_a(1-\rho)}. \tag{26}$$

The system exhibits a backward bifurcation, if equations Eq. (23) and Eq. (26) holds such that there is a possibility of multiple equilibrium states, thus, $R_0^a < 1$ is not a guarantee for disease eradication. Consequently, a forward bifurcation occurs if equations Eq. (24) and Eq. (26) holds demonstrating that $R_0^a < 1$ is sufficient for disease eradication [30]. Thus, a bifurcation diagram is illustrated in Figure 3. This result implies that the AFE exhibits a global asymptotic stability when $R_0^a < 1$, implying elimination of the disease. Conversely, when $R_0^a > 1$, the endemic equilibrium is globally asymptotically stable, indicating sustained transmission of amebiasis [31].

3.5. Global stability of the endemic equilibrium state of the amebiasis sub-model

We investigate the global stability of the endemic equilibrium E^{e*} to assess whether the system converges to this state for all admissible initial conditions within the feasible region. To establish this, we present and prove the following theorem.

Theorem 3.7. For $R_0^a > 1$, the endemic equilibrium state is globally asymptotically stable.

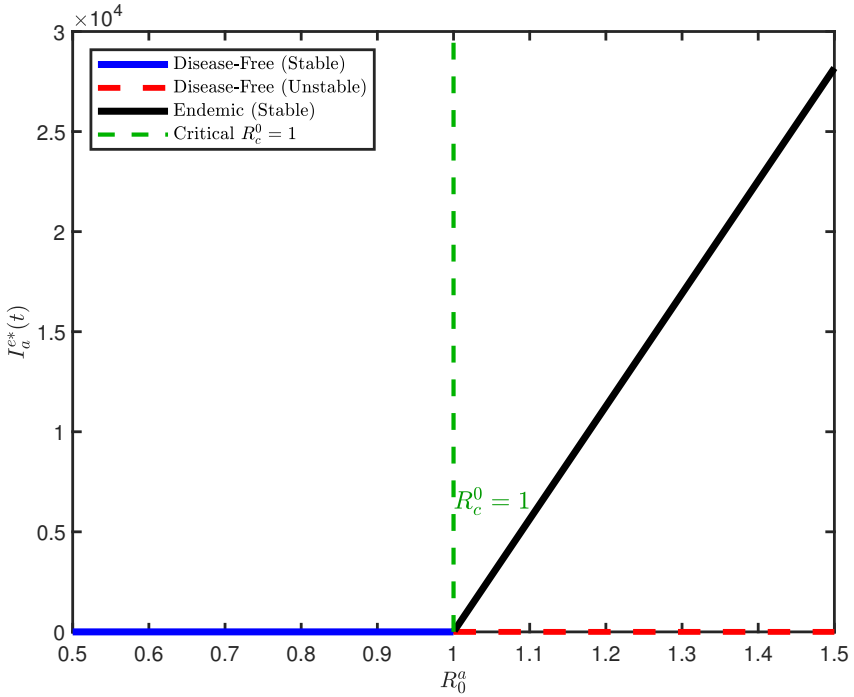


Figure 3: Bifurcation plot of amebiasis fever sub-model.

Proof. Let

$$V(X) = (S, I_a, R_a)^T.$$

Consider the Lyapunov function,

$$V(X) = \Big[S - S^{e*} - S^{e*} \ln \frac{S}{S^{e*}}\Big] + b_1\Big[I_a - I_a^{e*} - I_a^{e*} \ln \frac{I_a}{I_a^{e*}}\Big] + b_2\Big[R_a - R_a^{e*} - R_a^{e*} \ln \frac{R_a}{R_a^{e*}}\Big], \tag{27}$$

where b_1 and b_2 are unknown constants. Thus, equation Eq. (27) becomes

$$V' = \Big[1 - \frac{S^{e*}}{S}\Big]S' + b_1\Big[1 - \frac{I_a^{e*}}{I_a}\Big]I_a' + b_2\Big[1 - \frac{R_a^{e*}}{R_a}\Big]R_a'. \tag{28}$$

Let

$$\Lambda = -\kappa R_a^{e*} + (1-\rho)\beta_a I_a^{e*} S^{e*} + \mu S^{e*}, \quad (\psi + d_1 + u) = (1-\rho)\beta_a S^{e*}, \quad (\kappa + \mu) = \frac{\psi I_a^{e*}}{R_a^{e*}}. \tag{29}$$

Substituting equation Eq. (29) into equation Eq. (28) result in

$$\begin{aligned} V' = &-\mu\frac{(S - S^{e*})^2}{S} + \Big[1 - \frac{S^{e*}}{S}\Big]\Big[\kappa R_a^{e*}\Big(\frac{R_a}{R_a^{e*}} - 1\Big) + (1-\rho)\beta_a I_a^{e*} S^{e*}\Big(1 - \frac{S}{S^e}\frac{I_a}{I_a^{e*}}\Big)\Big] \\ &+ b_1\Big[1 - \frac{I_a^{e*}}{I_a}\Big]\Big[(1-\rho)\beta_a I_a^{e*} S^{e*}\Big(\frac{S}{S^{e*}}\frac{I_a}{I_a^{e*}} - 1\Big) + (1-\rho)\beta_a S^{e*} I_a^{e*}\Big(1 - \frac{I_a}{I_a^e}\Big)\Big] \\ &+ b_2\Big[1 - \frac{R_a^{e*}}{R_a}\Big]\Big[\psi I_a^{e*}\Big(\frac{I_a}{I_a^{e*}} - 1\Big) + \psi I_a^{e*}\Big(1 - \frac{R_a}{R_a^{e*}}\Big)\Big]. \end{aligned} \tag{30}$$

The coefficients of $\frac{S}{S^{e*}}$, $\frac{I_a}{I_a^{e*}}$, and $\frac{R_a}{R_a^{e*}}$ are selected to satisfy the conditions $b_1 = 1$, $b_2 = \frac{\kappa R_a^{e*}}{\psi I_a^{e*}}$ and $(1-\rho)\beta_a I_a^{e*} S^{e*} = 0$. Thus equation Eq. (30) becomes

$$V' = -\mu\frac{(S - S^{e*})^2}{S} + \kappa R_a^{e*}\Big[-\frac{R_a}{R_a^{e*}}\cdot\frac{S^{e*}}{S} + \frac{S^{e*}}{S} + \frac{I_a}{I_a^{e*}} - \frac{I_a}{I_a^{e*}}\cdot\frac{R_a^{e*}}{R_a}\Big] + (1-\rho)\beta_a S^{e*}\Big[2 - \frac{I_a}{I_a^{e*}} - \frac{I_a^{e*}}{I_a}\Big] \tag{31}$$

Let $v(x) = 1 - x > 0$, with equality attained only at $x = 1$. By the inequality $1 - x \le -\ln x$, it follows that the term κR_a^{e*} in equation Eq. (31) reduces to

$$\Big(1 - \frac{R_a}{R_a^{e*}}\cdot\frac{S^{e*}}{S}\Big) - \Big(1 - \frac{S^{e*}}{S}\Big) + \Big(1 - \frac{I_a}{I_a^{e*}}\cdot\frac{R_a^{e*}}{R_a}\Big) - \Big(1 - \frac{I_a}{I_a^{e*}}\Big) \le -\ln\frac{R_a}{R_a^{e*}}\cdot\frac{S^{e*}}{S} + \ln\frac{S^{e*}}{S}$$

$$-\ln\frac{I_a}{I_a^{e*}}\cdot\frac{R_a^{e*}}{R_a}+\ln\frac{I_a}{I_a^{e*}}=\ln\Big(\frac{S}{S^{e*}}\cdot\frac{R_a^{e*}}{R_a}\cdot\frac{S^{e*}}{S}\cdot\frac{R_a}{R_a^{e*}}\cdot\frac{I_a^{e*}}{I_a}\cdot\frac{I_a}{I_a^{e*}}\Big)=0.$$

Furthermore, by applying the arithmetic-geometric mean inequality to the term $(1-\rho)\beta_a S^{e*}$ in equation Eq. (31), we obtain zero. Consequently, equation Eq. (31) reduces to

$$V'=-\mu\frac{(S-S^{e*})^2}{S}\leq 0. \tag{32}$$

Applying LaSalle's invariance principle [33], we deduce that the solutions of the typhoid sub-model Eq. (21) converge to the endemic equilibrium whenever $R_0^a>1$ as $t\to\infty$. Consequently, the unique endemic equilibrium of the typhoid fever sub-model Eq. (21) is globally asymptotically stable. □

3.6. Typhoid fever–amebiasis (TFA) co-infection model

Stability of TFA-free equilibrium (TFAFE) and basic reproduction number, R_0

The feasible region of the full TFA co-infection system (1) is given by $\Pi_{TFA}=\frac{\Lambda}{\mu}$. The typhoid fever-amebiasis-free equilibrium (TFAFE) of the model is

$$E_0=(S,I_a,I_t,I_{at},R_a,R_t,R)=\Big(\tfrac{\Lambda}{\mu},0,0,0,0,0,0\Big).$$

The basic reproduction number of the co-infection model, denoted R_0, is the maximum of the reproduction numbers for the typhoid fever and amebiasis sub-systems, i.e.,

$$R_0=\max(R_0^t,R_0^a).$$

This is obtained using the next-generation matrix approach, with

$$F=\begin{pmatrix}(1-\rho)\beta_a S_0 & 0 & (1-\rho)\beta_a S_0\\ 0 & \rho\beta_a S_0 & \rho\beta_a S_0\\ 0 & 0 & 0\end{pmatrix},\quad V=\begin{pmatrix}f_1 & 0 & -\omega_1\\ 0 & f_2 & -\omega_2\\ 0 & 0 & f_3\end{pmatrix}.$$

$$V^{-1}=\begin{bmatrix}{f_1}^{-1} & 0 & \frac{\omega_1}{f_1 f_3}\\ 0 & {f_2}^{-1} & \frac{\omega_2}{f_2 f_3}\\ 0 & 0 & {f_3}^{-1}\end{bmatrix}$$

and

$$FV^{-1}=\begin{bmatrix}\frac{(1-\rho)\beta_a S_0}{f_1} & 0 & \frac{(1-\rho)\beta_a S_0\omega_1}{f_1 f_3}+\frac{(1-\rho)\beta_a S_0}{f_3}\\ 0 & \frac{\rho\beta_t S_0}{f_2} & \frac{\rho\beta_t S_0\omega_2}{f_2 f_3}+\frac{\rho\beta_t S_0}{f_3}\\ 0 & 0 & 0\end{bmatrix}.$$

Upon obtaining the spectral radius of FV^{-1}, we have $R_0^t=\dfrac{\rho\beta_t\Lambda}{\mu(\eta+d_2+\mu)}$ and $R_0^a=\dfrac{\Lambda(1-\rho)\beta_a}{\mu(\psi+d_1+\mu)}$.

Such that $R_0=max(R_0^t,R_0^a)$, where $f_1=\psi+d_1+\mu$, $f_2=\eta+d_2+\mu$, $f_3=\nu+d_3+\omega_1+\omega_2+\mu$. Also, based on the outcome of Theorem 3.2 and Theorem 3.5 as applied to typhoid fever and amebiasis systems, respectively, it is established that the E_0 of the typhoid fever-amebiasis system Eq. (1) is locally asymptotically stable if $R_0<1$ and unstable if $R_0>1$ [34]. This can be proved as follows: We address the DFE stability of system Eq. (1) since the next-generation approach is employed for the computation of R_0.

Theorem 3.8. *E_0 is locally asymptotically stable if $R_0<1$ and unstable if $R_0>1$.*

Proof. Theorem 3.8 implies that the typhoid fever-amebiasis co-infection can be eliminated over time if $R_0<1$ and this will be carried out using linearisation method by obtaining the Jacobian matrix, $J(E_0)$ of system of equations Eq. (1), given as follows:

$$J(E_0)=\begin{bmatrix}-\mu & -A\beta_a S_0 & -\rho\beta_t S_0 & -A\beta_a S_0-\rho\beta_t S_0 & \kappa & \tau & \alpha\\ 0 & A\beta_a S_0-f_1 & 0 & \omega_1 & 0 & 0 & 0\\ 0 & 0 & \rho\beta_t S_0-f_1 & \omega_2 & 0 & 0 & 0\\ 0 & 0 & 0 & -f_3 & 0 & 0 & 0\\ 0 & \psi & 0 & 0 & -f_4 & 0 & 0\\ 0 & 0 & \eta & 0 & 0 & -f_5 & 0\\ 0 & 0 & 0 & \nu & 0 & 0 & -f_6\end{bmatrix}.$$

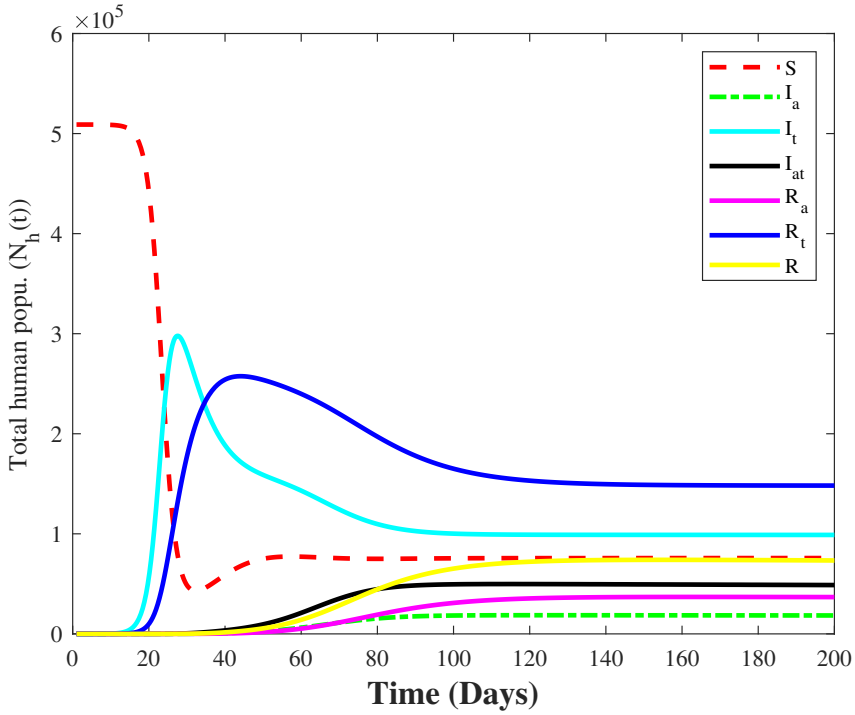


Figure 4: Plots of (a) $S, I_a, I_t, I_{at}, R_a, R_t,$ and R.

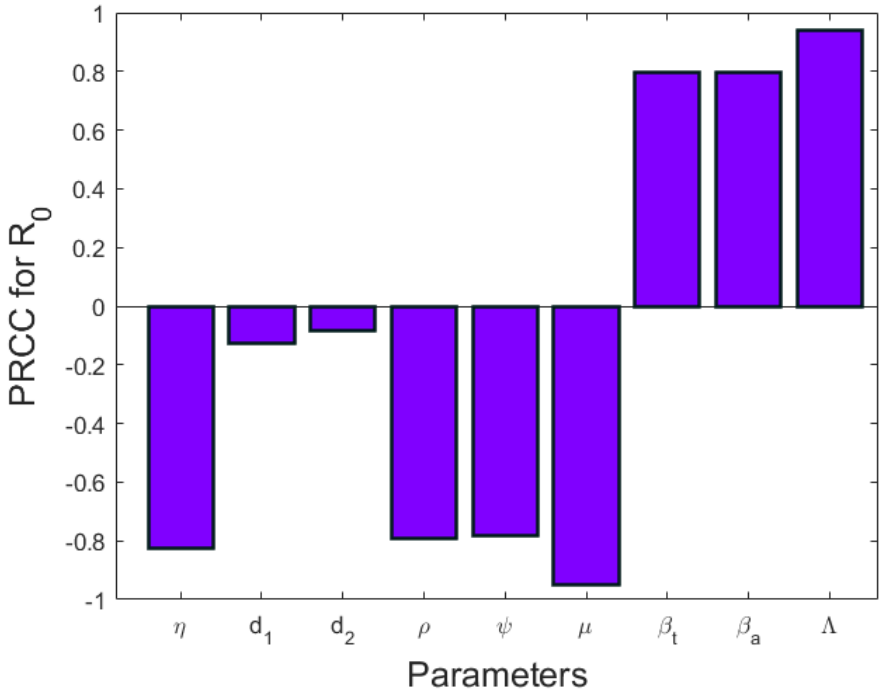
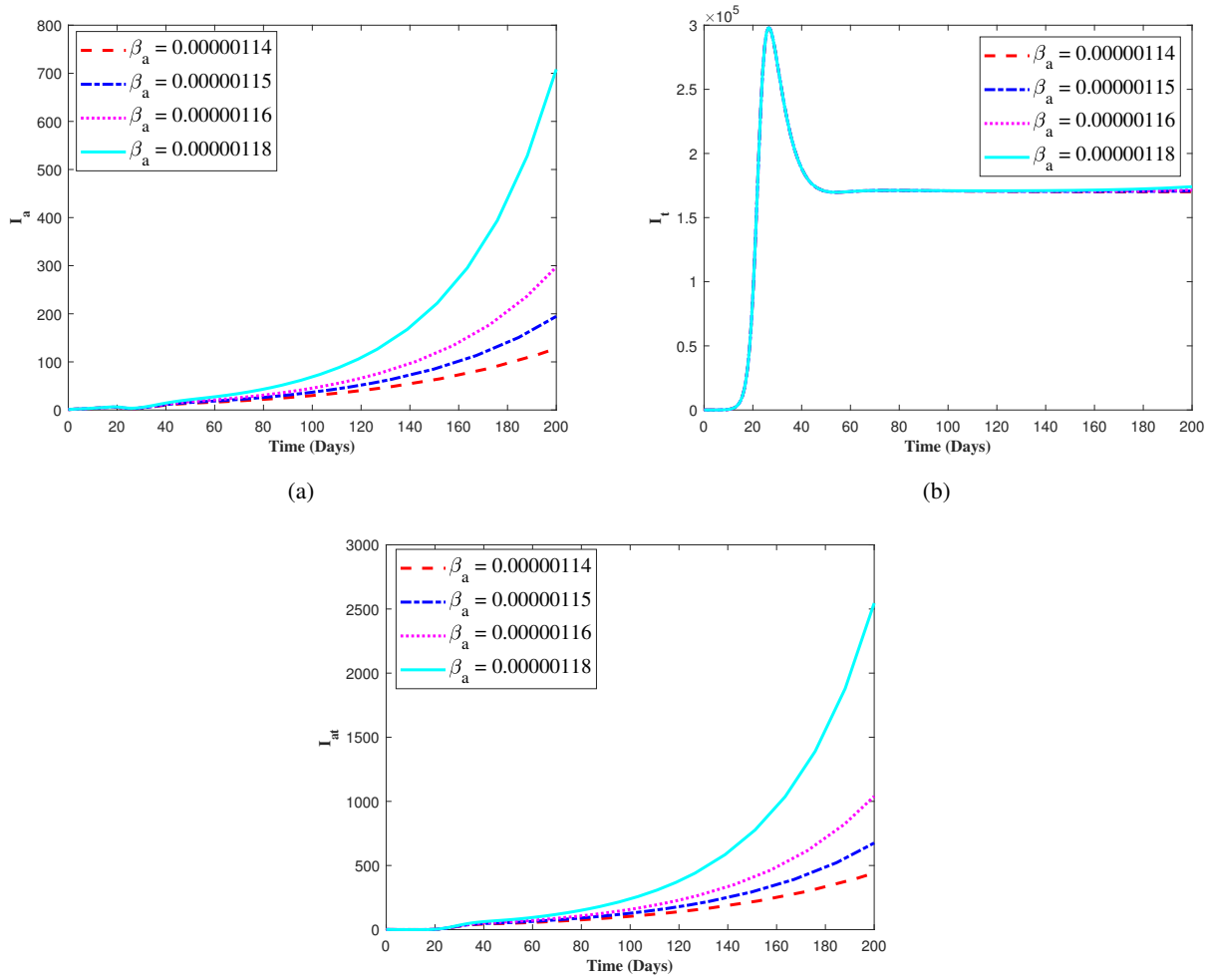


Figure 5: Partial rank correlation coefficient (PRCC) values illustrating the impact of parameters on R_0.

Applying the inspection method as used by [32], we have the eigenvalues, $\lambda_1, ..., \lambda_7$ as $\mu, -f_4, -f_5, -f_6, f_1(R_0^a - 1), f_2(R_0^t - 1), -f_3$, where $f_1 = (\psi + d_1 + \mu), f_2 = (\eta + d_2 + \mu), f_3 = (\nu + d_3 + \omega_1 + \omega_2 + \mu), f_4 = (\kappa + \mu), f_5 = (\tau + \mu), f_6 = (\alpha + \mu)$.
Since all the eigenvalues $\lambda_1, ..., \lambda_7$ are negative provided $R_0^a < 1$ and $R_0^t < 1$ it is evident that the system of equations Eq. (1) of the typhoid fever-amebiasis co-infection model is locally asymptotically stable. □

Table 2: Sensitivity indices of selected model parameters.

Parameters	Index signs	Sensitivity index values
β_t	+	0.7968
β_a	+	0.7957
Λ	+	0.9408
η	−	0.8275
d_1	−	0.1281
d_2	−	0.0820
ρ	−	0.7928
ψ	−	0.7843
μ	−	0.9474



(a) (b)

(c)

Figure 6: Varying values of β_a for (a) the infected and infectious population of amebiasis, (I_a), (b) the infected and infectious population of typhoid fever, (I_t), (c) co-infected and infectious population (I_{at}).

4. Numerical simulations

Typhoid fever-amebiasis co-infection is widespread in many countries in Africa, like Nigeria and specifically Benue State, due to their shared transmission route [1, 4, 6]. Whether occurring individually or concurrently, both diseases pose major public health challenges, highlighting the need for targeted interventions and effective control measures. For numerical simulations of these co-infections, it is crucial to evaluate parameter values that approximate real-world situations, despite the lack of empirical data. Such estimates enable the generation of contextually relevant results for Nigeria, particularly Makurdi, Benue State.

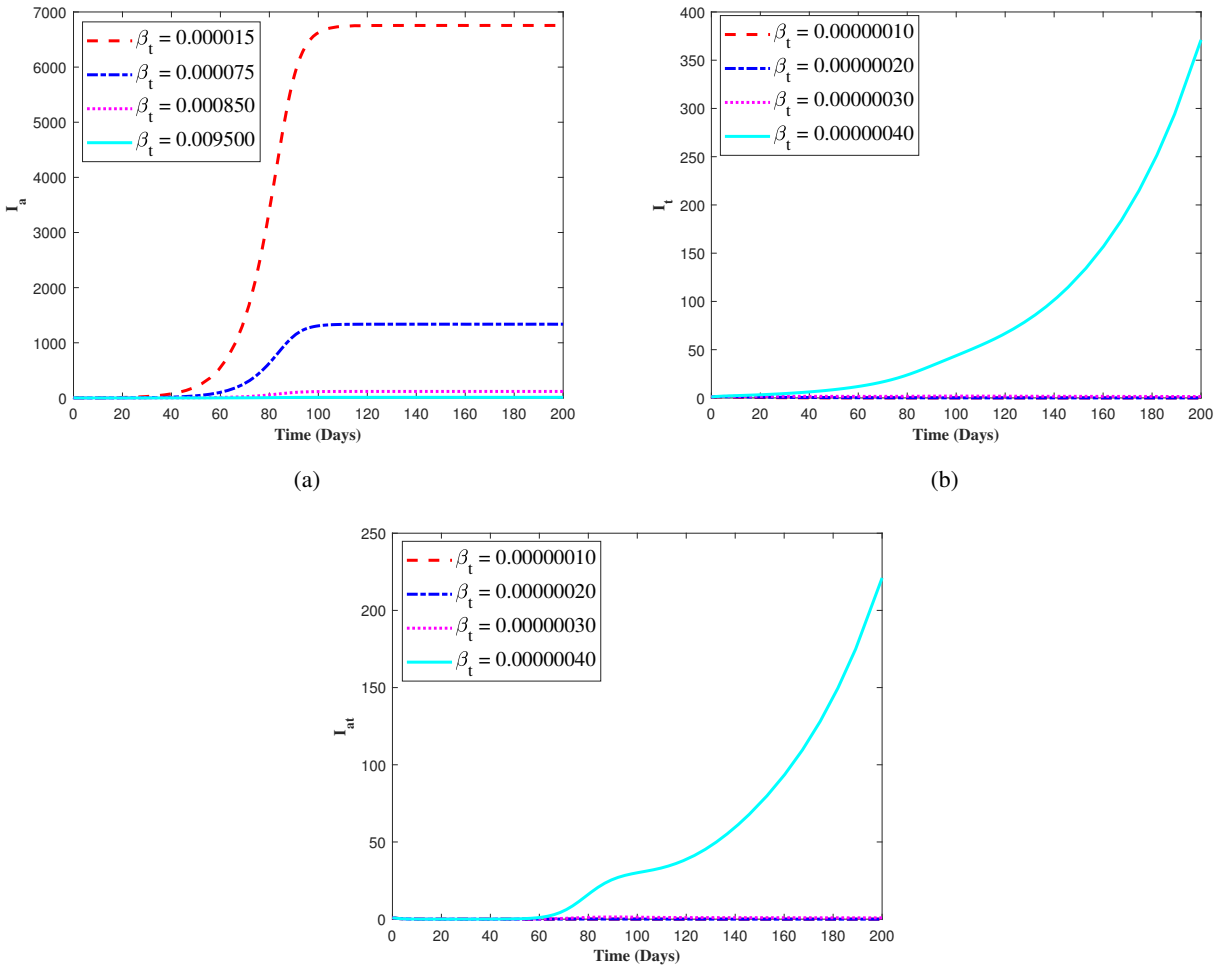


Figure 7: Varying values of β_t for (a) the infected and infectious population of amebiasis, (I_a), (b) the infected and infectious population of typhoid fever, (I_t), (c) co-infected and infectious population (I_{at}).

4.1. Parameter estimation

Parameter values were estimated to facilitate numerical analysis of TFA co-dynamics for accurate forecasting as well as prediction. All estimated values were expressed in days, using demographic data from Makurdi, Benue State, Nigeria. The population of Makurdi is $S^0 = 509{,}000$, with an average life expectancy of approximately 56 years. The natural death rate is therefore

$$\mu = \frac{1}{\text{Life expectancy}} = \frac{1}{56 \times 365} \approx 0.000049 \text{ per day.}$$

The demographic sources are given in Refs. [25, 35]. Since $S^0 = \frac{\Lambda}{\mu}$, the recruitment rate is estimated as

$$\Lambda = 0.000049 \times 509{,}000 \approx 25 \text{ per day.}$$

The mortality rate related to disease for co-infected individuals, d_3, was taken as the sum of d_1 and d_2, reflecting the elevated mortality risk from dual infection, yielding $d_3 = 0.000341$. Ref. [23] indicates that amebiasis can be treated within 5 to 10 days. Using the average duration, $\psi = \frac{1}{7.5} = 0.133$ is obtained. Similarly, $\omega_2 = 0.133$ is derived for treatment and recovery from amebiasis in the co-infected class, and $\omega_1 = 0.1$ is calculated using the same approach. The parameter ν is estimated as 0.1, since 7.5 days falls within the 10-day range, resulting in $\nu = 0.1$. Furthermore, Refs. [1, 3, 4, 6] report that there is no permanent immunity for either disease after recovery, so individuals may become susceptible to one or both diseases within days or months, depending on hygiene practices and preventive measures. Due to the poor hygiene practices observed in the studied population in Makurdi, as noted by Maxwell *et al.* [8], possibility of reinfection is assumed to occur, on average, 15 days after recovery. This assumption leads to $\tau = \frac{1}{15} = 0.0667$,

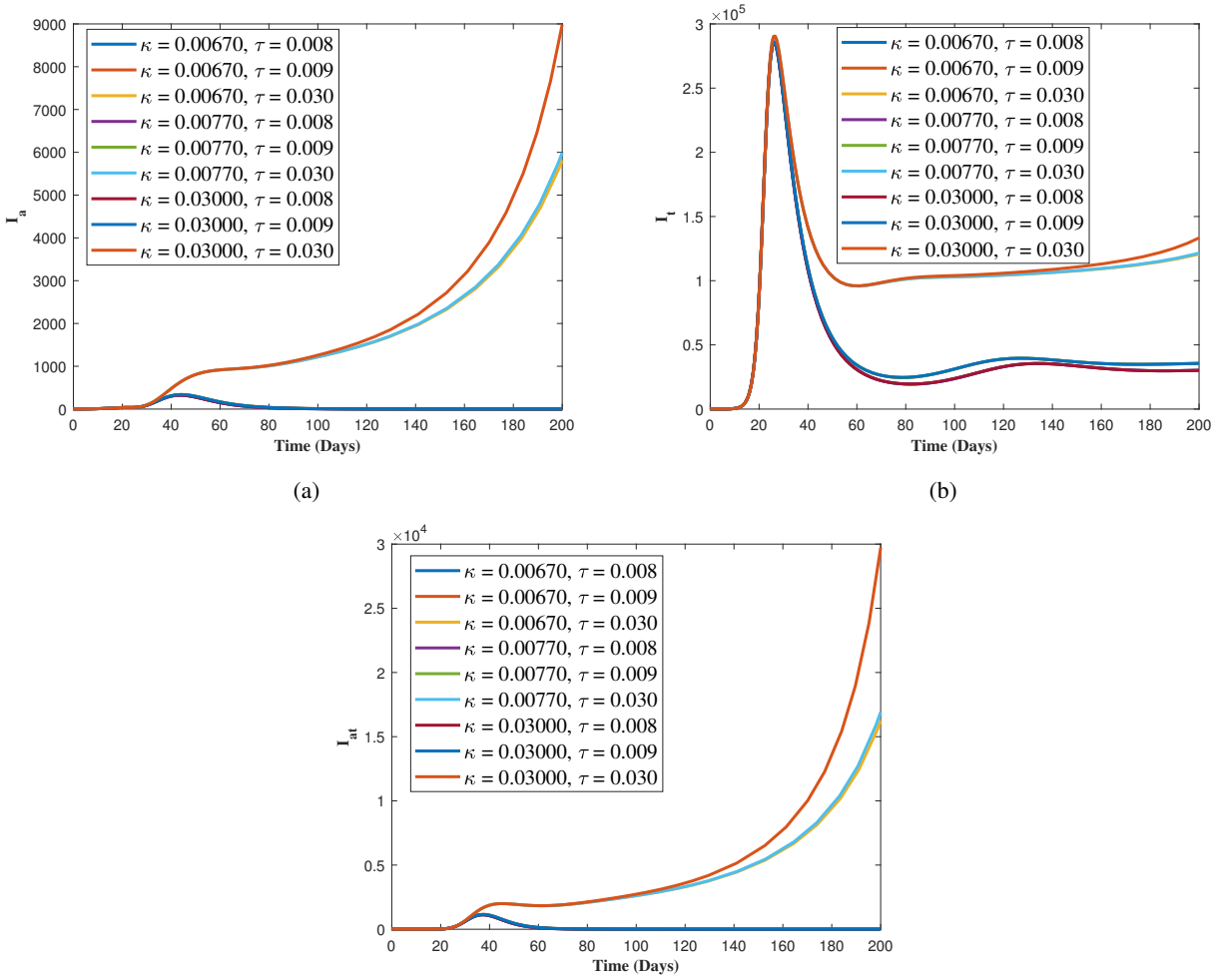


Figure 8: Varying values of κ and τ for (a) the infected and infectious population of amebiasis, (I_a), (b) the infected and infectious population of typhoid fever, (I_t), (c) co-infected and infectious population (I_{at}).

$\kappa = \frac{1}{15} = 0.0667$, and the same value is assigned to α, resulting in $\alpha = 0.0667$. Table 1 presents details of other parameters. Then we utilised

$$I_{a0} = 1,\ I_{t0} = 1,\ I_{at0} = 1,\ R_{a0} = 0,\ R_{t0} = 0,\ R(0) = 0,\ S_0 = 508{,}997,$$

for the simulations, where S_0 was obtained after deducting the infected compartments.

4.2. Baseline plots

Numerical simulations are conducted for each equation in system Eq. (1) using details provided in Table 1 and $(S, I_a, I_t, I_{at}, R_a, R_t, R) = (508997, 1, 1, 1, 0, 0, 0)$. This approach was employed to assess the co-dynamics of both diseases in the population and to inform decision-making and resource allocation for effective disease control.

Figure 4 illustrates the baseline simulation for each individual class of Eq. (1). Susceptible population, S declines from approximately 509,000 on day 18 to about 47,528 on day 30, and further to 75,776 by day 200, reflecting infections with typhoid fever and amebiasis.

The I_t curve in Figure 4 illustrates the dynamics of individuals infected solely with typhoid fever, rising from about day 15 to approximately 297,352 by day 27 before declining to a stable level of about 98,889 by day 200. This reduction likely reflects the impact of screening and treatment. The I_a curve shows that the amebiasis-infected population grows at a slower rate and remains smaller than the typhoid-infected population, indicating that typhoid fever spreads more rapidly and with greater prevalence. It starts increasing from about day 50 and maintain a steady state of about 18,408 till day 200. Similarly, the I_{at} curve represents the co-infected population, which begins to increase around day 30 and stabilizes at approximately 48,787 by day 200. These results suggest that co-infection is less prevalent than typhoid fever alone, but its dynamics warrant careful consideration.

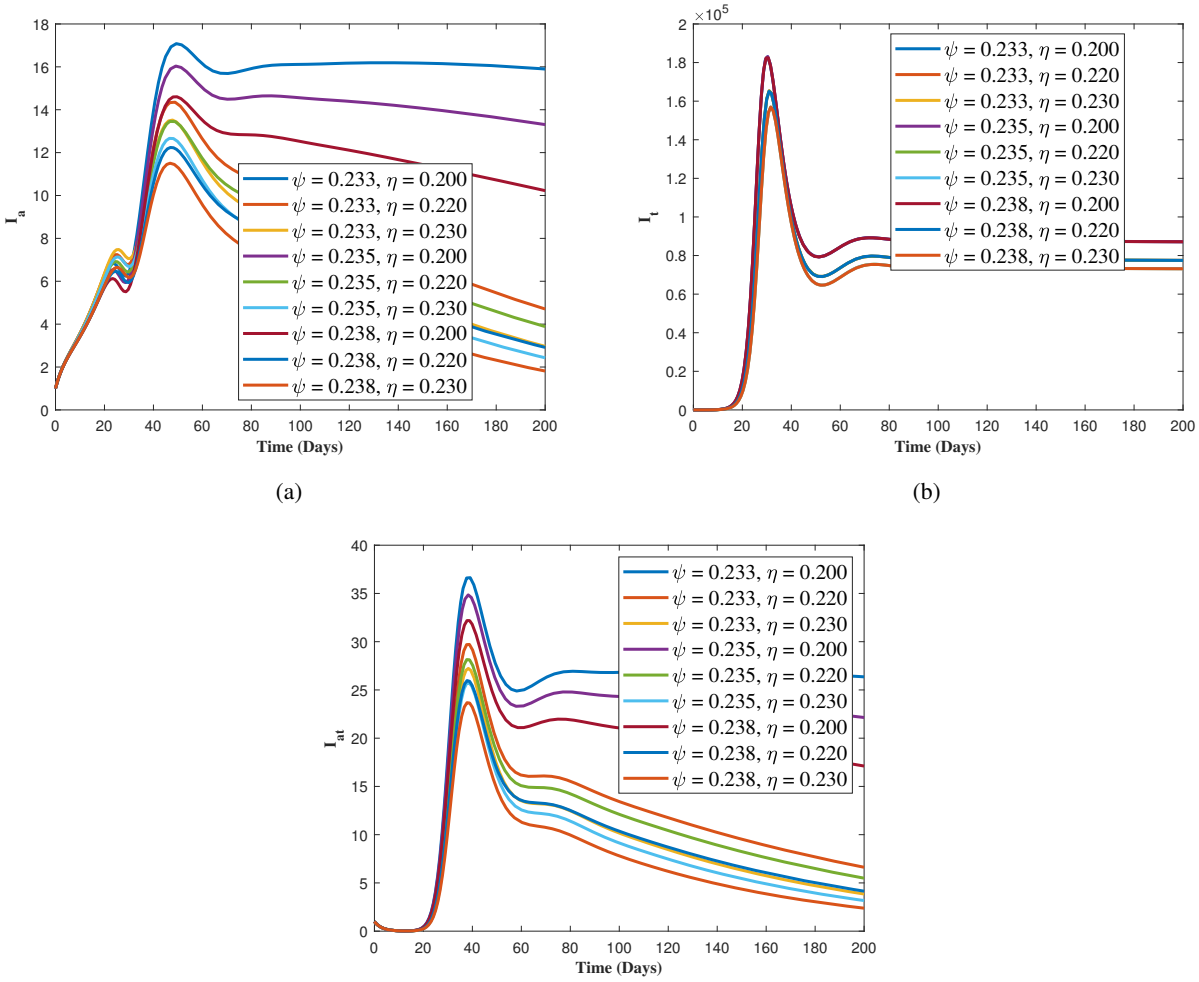


Figure 9: Varying values of ψ and η for (a) the infected and infectious population of amebiasis, (I_a), (b) the infected and infectious population of typhoid fever, (I_t), (c) co-infected and infectious population (I_{at}).

The R_t, R_a, and R_{at} curves in Figure 4 depict the recovery patterns of individuals infected with typhoid fever, amebiasis, and both diseases, respectively. The comparatively higher recovery rate among typhoid fever cases may be attributed to greater disease awareness and more widespread screening and treatment efforts.

4.3. Global sensitivity analysis

Global sensitivity analysis was carried out via Partial Rank Correlation Coefficient (PRCC) with Latin Hypercube Sampling (LHS) to evaluate the relative importance of parameters in the transmission dynamics of typhoid-amebiasis co-infection, based on the values in Table 1. The analysis employed the basic reproduction numbers as described in [16, 36]. Parameters with positive PRCC values increase the reproduction number and thereby promote disease spread, while those with negative values reduce it. Parameters with $PRCC \geq 0.5$ or $PRCC \leq -0.5$ are considered highly influential, whereas those with $PRCC < 0.5$ or $PRCC > -0.5$ are less influential but still contribute to transmission. The PRCC plots for the respective reproduction numbers are presented in Figure 5. This analysis highlights how parameter variations shape disease dynamics and co-infection risks, providing insights to guide decision-making and resource allocation for effective control. The plot was generated using 1000 runs and a 95% confidence interval. The parameter range examined spans from 0.9 to 1.1.

An increase in the parameters Λ, β_t, and β_a raises the basic reproduction number, thereby facilitating the spread of typhoid fever, amebiasis, or their co-infection. Specifically, the recruitment rate (Λ), the typhoid fever contact rate (β_t), and the amebiasis contact rate (β_a) exert strong influence on transmission. This implies that to reduce the reproduction number and, by extension, the spread of these diseases, either individually or as a co-infection, these three parameters require effective control. Conversely, higher values of the progression rate from I_a to R_a through screening and treatment (ψ), the progression rate from I_t to R_t through screening and treatment (η), the natural death rate (μ), the proportion of individuals infected with typhoid fever (ρ), and the disease-induced

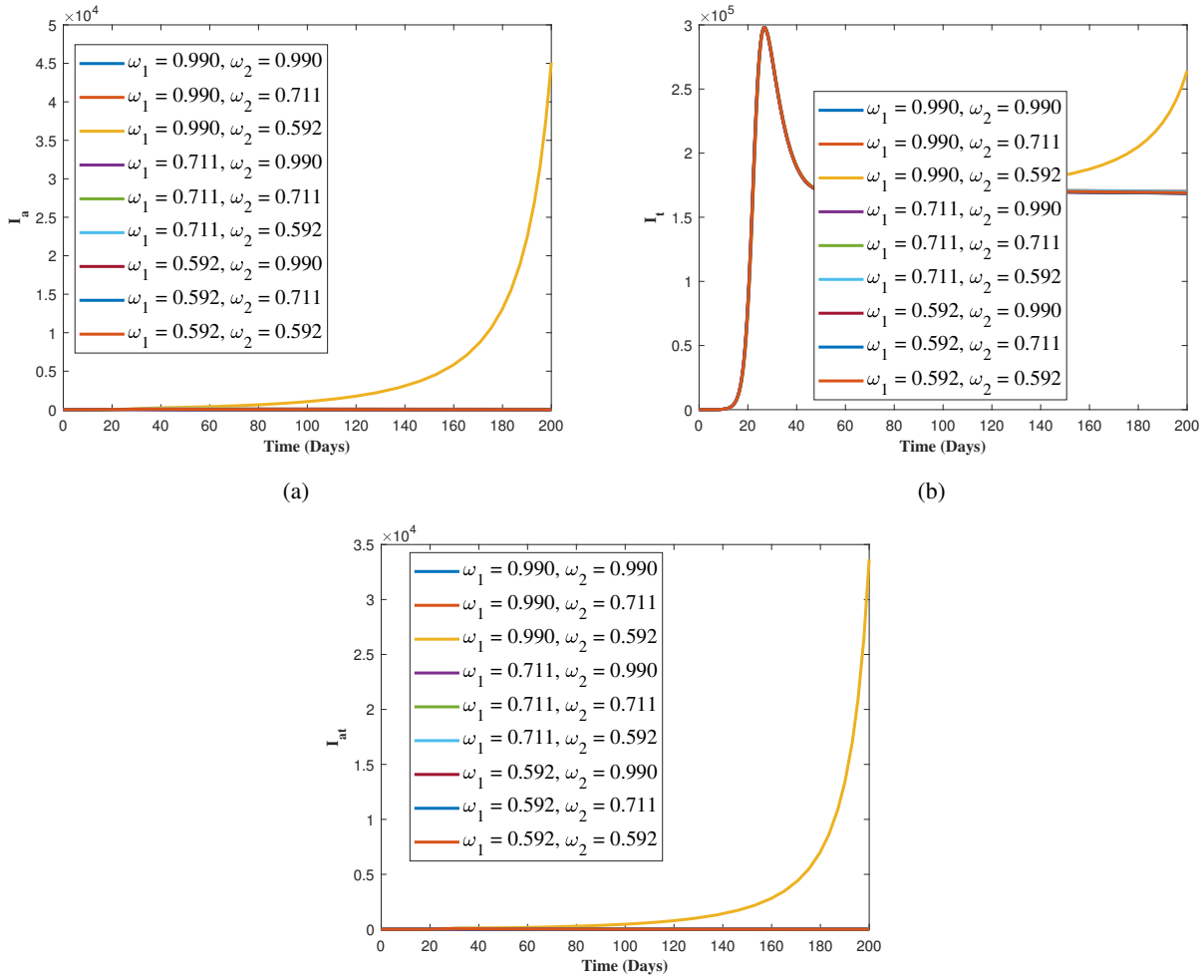


Figure 10: Varying values of ω_1 and ω_2 for (a) the infected and infectious population of amebiasis, (I_a), (b) the infected and infectious population of typhoid fever, (I_t), (c) co-infected and infectious population (I_{at}).

death rates (d_1, d_2) are associated with reduced transmission. Among these, ψ, η, and μ are the most impactful in lowering disease spread. Furthermore, as ρ increases, typhoid fever transmission intensifies while amebiasis infection declines, thereby reducing the prevalence of co-infection. In summary, as these parameters increases, the reproduction number decreases, thereby leading to the reduction of the diseases in the population. The details of the PRCC values are shown in Table 2

4.4. Simulations

Figure 6 shows that an increase in β_a causes an increase in the I_a and I_{at} classes, with a reduction in the I_t class, implying that amebiasis becomes more dominant than typhoid fever in the modelled population.

In Figure 7, an increase in β_t causes an increase in the I_t class, with reductions in the I_a and I_{at} classes.

As seen in Figure 8, an increase in κ and an increase in τ lead to higher values in the I_a, I_t, and I_{at} compartments, indicating that greater loss of immunity contributes to increased prevalence of amebiasis and typhoid fever in the population.

A reduction in ψ and an increase in η lead to lower values in the I_a, I_{at}, and a reduction in I_t compartments as shown in Figure 9.

Figure 10 shows that an increase in ω_1 coupled with a reduction in ω_2 favours the growth of the amebiasis-only class (I_a), indicating that conditions promoting amebiasis transmission while limiting typhoid spread shift the burden toward amebiasis. Conversely, a decrease in ω_1 with an increase in ω_2 drives expansion of the typhoid-only class (I_t), reflecting stronger typhoid transmission relative to amebiasis. When both ω_1 and ω_2 rise simultaneously, the co-infected class (I_{at}) expands.

5. Discussion

Findings indicate that the rapid spread of typhoid fever may reduce the pool of susceptible individuals or prompt behavioural changes, such as improved hygiene, which indirectly limit opportunities for amebiasis transmission [10]. Likewise, intensified public health measures targeting rising amebiasis cases can curb typhoid fever through shared transmission pathways. Thus, rather than mutually amplifying, the two infections interact competitively where the dominance of one constrains the prevalence of the other, underscoring the need for integrated control strategies that address this epidemiological interplay [8].

As immunity to both diseases wanes, the susceptible pool is replenished more quickly, leaving previously protected individuals vulnerable again. This recurring cycle drives higher reinfection rates, enlarging the infected populations and amplifying transmission opportunities. The result is compounded co-infection burdens, more frequent immune challenges, heightened inflammation, and increased risk of complications. Such dynamics create a feedback loop in which accelerated immunity loss undermines control efforts and sustains elevated prevalence, emphasizing the need for integrated interventions that disrupt reinfection cycles and reinforce long-term immunity or treatment adherence. These include proper water, sanitation, and hygiene (WASH) practices such as using safe, clean drinking water, appropriate dispersal of human waste, regular handwashing with soap, safe food handling, and maintaining a clean environment.

Since screening and treatment slow recovery from typhoid but accelerate recovery from amebiasis, typhoid infections persist longer, sustaining transmission and enlarging its compartment, while amebiasis clears more quickly, reducing its compartment. This imbalance expands the co-infection class, as individuals with prolonged typhoid infection remain infectious and are more likely to acquire or sustain amebiasis before recovery. Overall, the dynamics show how differential treatment effectiveness and recovery rates can shift infection burdens: extended persistence of one disease promotes co-infection prevalence even as the other declines. This underscores the need for coordinated interventions that balance treatment outcomes across both pathogens to prevent unintended increases in co-infection.

Findings show that the relative progression rates from the co-infection class to either typhoid or amebiasis determine which pathway dominates, with intensified transmission routes for both diseases increasing the likelihood of dual infections. This indicates that interventions targeting only one disease may inadvertently shift the infection burden toward the other or elevate co-infection prevalence, highlighting the need for integrated strategies that balance both transmission pathways.

6. Conclusion

Direct human-to-human transmission of typhoid fever and amebiasis is particularly challenging in endemic regions. This study examined their co-infection dynamics, revealing that an average increase in the progression rate of co-infected individuals to either the typhoid or amebiasis class ultimately enlarges the co-infected compartment over time.

In this study, we computed the disease-free and endemic equilibrium states for the sub-models. The forward bifurcation confirmed that $R_0 < 1$ constitutes the necessary and sufficient condition for disease elimination [30]. Numerical simulations showed that increased immunity loss enlarges the co-infected class, while higher transmission rates in either typhoid or amebiasis reduce the prevalence of the other. PRCC analysis was conducted to assess parameter influence on disease dynamics. Overall, the results indicate that effective prevention, screening, and treatment are essential to control each disease and their co-infection. Future work would focus on incorporating environment-to-human (indirect) transmission pathways, using real-world data for model calibration and parameter estimation, accounting for population heterogeneity, and implementing optimal control and cost-effectiveness analyses. Identifying the most suitable and cost-effective control strategies is particularly important given resource constraints.

Data availability

All the Data (parameter values) used in this work have been cited appropriately in Table 1.

Declaration of competing interest

The authors declare that they have no known competing financial interests or personal relationships that could have appeared to influence the work reported in this manuscript.

Funding

The authors received no specific funding from any public, commercial, or not-for-profit organisation for this research.

References

[1] World Health Organization, "Typhoid", 2023. Available online: https://www.who.int/news-room/fact-sheets/detail/typhoid.

[2] Centers for Disease Control and Prevention, "About typhoid fever and paratyphoid fever", 2024. Available online: https://www.cdc.gov/typhoid-fever/about/index.html.

[3] Centers for Disease Control and Prevention, "Clinical overview of typhoid fever and paratyphoid fever", 2024. Available online: https://www.cdc.gov/typhoid-fever/hcp/clinical-overview/index.html.

[4] Centers for Disease Control and Prevention, "Amebiasis", 2025. Available online: https://www.cdc.gov/amebiasis/about/index.html.

[5] A. Kawashima, Y. Yanagawa, R. Shimogawara, K. Yagita, H. Gatanaga & K. Watanabe, "Amebiasis as a sexually transmitted infection: A re-emerging health problem in developed countries", Global Health & Medicine **5** (2023) 319. https://doi.org/10.35772/ghm.2023.01064.

[6] F. M. S. Oliveira, A. C. C. Fernandes, S. H. C. Sandes, L. O. Prata, M. Abatemarco Jr., C. A. V. da Silva, G. H. Campolina-Silva, M. L. de J. Oliveira, C. A. Oliveira, E. Neumann, A. C. Nunes, M. A. Gomes & M. V. Caliari, "Co-infection by Salmonella enterica subsp. enterica serovar Typhimurium and Entamoeba dispar pathogenic strains enhances colitis and the expression of amoebic virulence factors", Microbial Pathogenesis **158** (2021) 105010. https://doi.org/10.1016/j.micpath.2021.105010.

[7] D.-A. T. Shirley, K. Watanabe & S. Moonah, "Significance of amebiasis: Ten reasons why neglecting amebiasis might come back to bite us in the gut", PLoS Neglected Tropical Diseases **13** (2019) e0007744. https://doi.org/10.1371/journal.pntd.0007744.

[8] O. Maxwell, A. Oklo & A. Bernard, "Profile of water related diseases in Benue State, Nigeria", American Journal of Human Ecology **1** (2012) 87. Available online: http://www.worldscholars.org/index.php/ajhe/article/viewFile/192/112.

[9] G. T. Jombo, E. M. Mbaawuaga, U. Ahmed, O. P. Abba & J. O. Tsor, "Management of typhoid fever at a university hospital in Sub-Saharan Africa: Challenges and prospects", International Journal of Health Sciences & Research **9** (2019) 190. Available online: https://www.ijhsr.org/IJHSR_Vol.9_Issue.1_Jan2019/29.pdf.

[10] M. O. Iboyi, N. G. Imandeh & E. T. Azua, "Prevalence and associated pre-disposing factors of amoebiasis among school children in Makurdi Metropolis, Benue State, Nigeria", Journal of Advances in Microbiology **5** (2017) 1. https://doi.org/10.9734/JAMB/2017/36609.

[11] H. Abboubakar & R. Racke, "Mathematical modelling and optimal control of typhoid fever", Konstanzer Schriften in Mathematik **386** (2019). Available online: https://www.math.uni-konstanz.de/~racke/dvidat/m2019-5.pdf.

[12] G. Zaman, I. H. Jung, D. F. M. Torres & A. Zeb, "Mathematical modelling and control of infectious disease", Computational and Mathematical Methods in Medicine **2017** (2017) 7149154. https://doi.org/10.1155/2017/7149154.

[13] S. Nana-Kyere, J. K. K. Asamoah, J. D.-G. Ankamah, E. Okyere, B. Seidu, D. Kwarteng, E. L. Ayetey & J. K. Odum, "Mathematical modeling and cost-effectiveness analysis of an $S_eE_eI_eR_e$ typhoid fever model", Journal of Mathematics **2025** (2025) 1212057. https://doi.org/10.1155/jom/1212057.

[14] I. U. Khan, S. Mustafa, A. Shokri, S. Li, A. Akgul & A. Bariq, "The stability analysis of a nonlinear mathematical model for typhoid fever disease", Scientific Reports **13** (2023) 15284. https://doi.org/10.1038/s41598-023-42244-5.

[15] A. K. Suhuyini & B. Seidu, "A mathematical model on the transmission dynamics of typhoid fever with treatment and booster vaccination", Frontiers in Applied Mathematics and Statistics **9** (2023) 1151270. https://doi.org/10.3389/fams.2023.1151270.

[16] K. A. Tijani & C. E. Madubueze, "Understanding the dynamics of amebiasis using mathematical modelling approach: Optimal control strategies and cost-effectiveness analysis", International Journal of Mathematical Sciences and Optimization: Theory and Applications **11** (2025) 138. https://doi.org/10.5281/zenodo.17604865.

[17] S. C. Mpeshe, "Fuzzy SEIR epidemic model of amoebiasis infection in human", Advances in Fuzzy Systems **2022** (2022) 5292830. https://doi.org/10.1155/2022/5292830.

[18] S. Edward & G. E. Mpogolo, "Modeling and optimal control of the transmission dynamics of amebiasis", Results in Control and Optimization **13** (2023) 100325. https://doi.org/10.1016/j.rico.2023.100325.

[19] F. Hategekimana, S. Saha & A. Chaturvedi, "Dynamics of amoebiasis transmission: Stability and sensitivity analysis", Mathematics **5** (2017) 58. https://doi.org/10.3390/math5040058.

[20] R. Adrizain, Aprimadhansari, V. Indriasari, D. D. Kusmayadi & D. Setiabudi, "Secondary infection of amoeba and typhoid fever in severe malnourished paediatric patient with type I choledochal cyst: A case report", Oxford Medical Case Reports **2020** (2020) omaa111. https://doi.org/10.1093/omcr/omaa111.

[21] J. Singh, R. Panneerselvam, S. Sundaramurthi, V. Chellappa & S. Sathasivam, "Salmonella enterica and Entamoeba histolytica co-infection presenting as multiple liver abscesses in an immunocompetent patient", International Surgery Journal **12** (2025) 462. https://doi.org/10.18203/2349-2902.isj20250593.

[22] H. O. Nyaberi & J. S. Musaili, "Mathematical modeling of the impact of treatment on the dynamics of typhoid", Journal of the Egyptian Mathematical Society **29** (2021) 15. https://doi.org/10.1186/s42787-021-00125-8.

[23] D. Bento & R. L. Austin, "Amebiasis", in StatPearls [Internet], StatPearls Publishing, Treasure Island, FL, USA, 2026. Available online: https://www.ncbi.nlm.nih.gov/books/NBK557718/.

[24] Cleveland Clinic, "Typhoid fever", 2026. Available online: https://my.clevelandclinic.org/health/diseases/17730-typhoid-fever.

[25] Macrotrends, "Nigeria life expectancy (1950–2025)", 2025. Available online: https://www.macrotrends.net/global-metrics/countries/nga/nigeria/life-expectancy.

[26] J. M. Mutua, F. B. Wang & N. K. Vaidya, "Modelling malaria and typhoid fever co-infection dynamics", Mathematical Biosciences **264** (2015) 128. https://doi.org/10.1016/j.mbs.2015.03.014.

[27] P. van den Driessche & J. Watmough, "Reproduction numbers and sub-threshold endemic equilibria for compartmental models of disease transmission", Mathematical Biosciences **180** (2002) 29. https://doi.org/10.1016/S0025-5564(02)00108-6.

[28] A. Amir, A. Ahmad, S. Zeb, S. A. M. Yatim & F. A. Abdullah, "A delay differential approach with sensitivity analysis for tuberculosis transmission and control", African Scientific Reports **5** (2026) 565. https://doi.org/10.46481/asr.2026.5.2.565.

[29] C. Castillo-Chavez, Z. Feng & W. Huang, "On the computation of R_0 and its role on global stability", in Mathematical Approaches for Emerging and Reemerging Infectious Diseases: An Introduction, C. Castillo-Chavez, S. Blower, P. van den Driessche, D. Kirschner & A. A. Yakubu (Eds.), Springer, New York, NY, USA, 2002, pp. 229–250. Available online: https://www.researchgate.net/publication/228915276.

[30] A. Abokwara & C. E. Madubueze, "Optimizing the control of lymphatic filariasis: A mathematical modelling and cost-effectiveness analysis", Discover Public Health **22** (2025) 703. https://doi.org/10.1186/s12982-025-01058-8.

[31] C. Castillo-Chavez & B. Song, "Dynamical models of tuberculosis and their applications", Mathematical Biosciences and Engineering **1** (2004) 361. https://doi.org/10.3934/mbe.2004.1.361.

[32] K. A. Tijani, C. E. Madubueze, R. I. Gweryina & T. Aboiyar, "Mathematical modelling and optimal-control strategies of schistosomiasis–typhoid fever co-infection: Using the demographic setting of Makurdi, Benue State, Nigeria", Journal of the Nigerian Society of Physical Sciences **8** (2026) 3376. https://doi.org/10.46481/jnsps.2026.3376.

[33] J. P. LaSalle, *The Stability of Dynamical Systems*, SIAM, Philadelphia, PA, USA, 1976. https://doi.org/10.1137/1.9781611970432.

[34] R. I. Gweryina, C. E. Madubueze, V. P. Bajiya & F. E. Esla, "Modeling and analysis of tuberculosis and pneumonia co-infection dynamics with cost-effective strategies", Results in Control and Optimization **10** (2023) 100210. https://doi.org/10.1016/j.rico.2023.100210.

[35] Macrotrends, “Makurdi, Nigeria metro area population (1950–2026)”, 2026. Available online: https://www.macrotrends.net/global-metrics/cities/23539/makurdi/population.

[36] S. Marino, I. B. Hogue, C. J. Ray & D. E. Kirschner, “A methodology for performing global uncertainty and sensitivity analysis in systems biology”, Journal of Theoretical Biology **254** (2008) 178. https://doi.org/10.1016/j.jtbi.2008.04.011.